PEOPULE'S DEMOCRATIC REPUBLIC OF ALGERIA
Higher Education and Scientific Research Ministry

University of Echahid Hamma Lakhdar- El-oued
Faculty of Exact Sciences

N° d'ordre :
N° de série :

A Dissertation Submitted to the Department of Physics

In Partial Fulfillment of the Requirements

For the Degree of Master in

Applied Physics Radiation and Energy

By**: Salma TEDJANI**

Title

Calculation of the oxygen rate in the $Ca_{1-x}Sr_xFeO_{2.5+y}$ compounds

Discussed on 25/05/2016

Members of jury:

Widad LAIADI	MCB	University of El-Oued	President
Ghani RIHIA	MAA	University of El-Oued	Examiner
Mohammed Sadok MAHBOUB	MCA	University of El-Oued	Supervisor

University season: 2015/2016

Dedication :

To...

My mother & father;

My brothers & sisters;

My grandmother;

My fiance "Imad";

And

Anyone who knows me…

.. Salma ..

Acknowledgements

First of all, I would like to express my sincere gratitude to my supervisor Dr. Mohammed Sadok MAHBOUB for all his support and encouragement. His ideas and suggestions were extremely useful to get this thesis its final shape. I feel lucky to work with him.

I am really grateful to the commission members: Mrs. Widad LAIADI and Mr. Ghani RIHIA for accepting to discuss my work. It is an honor for me.

I would like to thank Mr. Imad KHALDI communications engineer; Mr. Mohammed salah BOUHAMED Food engineer and Mr. Ahmed MERAD secondary teacher in "Bouchoucha" secondary school for their support to finish this work.

Salma TEDJANI

Table of contents

Chapter II: Characterization techniques

Chapter III: The oxygen rate in the $Ca_{1-x}Sr_xFeO_{2.5+y}$ compounds (x=0.5; 0.7; 0.9)

List of figures

List of tables

Nomenclature

Latin letters

a:	One of crystal lattice modes[Å]
A:	Cation
a_p:	The unit-cell edge of the perovskite subcell
APF_{exp}:	The experimental atomic packing factor
APF'_{exp}:	The supposed experimental atomic packing factor
APF_{theo}:	The theoretical atomic packing factor
b:	One of crystal lattice modes[Å]
b:	Axis
B:	Cation
c:	One of crystal lattice modes[Å]
C:	The light speed[m/s]
d_{hkl} :	The retinal distance between the crystalline levels[Å]
E :	Photon energy[J]
h:	Planck constant[J.s]
n:	Reflection order
nCa :	The Ca atoms number
n_i :	The atoms number
nFe1 :	The Fe atoms number in the tetrahedral sites
nFe2 (+3) :	The third Fe atoms number in the octahedral sites
nFe2 (+4) :	The fourth Fe atoms number in the octahedral sites
nSr :	The Sr atoms number
nO :	The O atoms number
N :	The number of information used(measuring points)
O :	Octahedral layers
P :	The number of refined parameters
r:	Ionic radii[Å]

r_A:	The A ionic radii[Å]
r_B:	The B ionic radii[Å]
rCa:	The Ca ionic radii[Å]
rFe1(T):	The Fe ionic radii in the tetrahedral sites[Å]
rFe2 +3 (O):	The third ionic radii in the octahedral sites [Å]
rFe2 +4 (O) :	The fourth ionic radii in the octahedral sites[Å]
r_O:	The O ionic radii[Å]
R:	radius of Debye-Scherrer film[m]
R_{exp} :	R- expected pattern
R_p :	R- pattern
R_{wp} :	R- weighted pattern
s :	The distance between two identical lines on Debye-Scherrer film[m]
t:	Tolerance factor
T :	Tetrahedral layers
V :	The total volume of the cell
w_i :	The Statistical weight and represents the contrast between the experimental and theoretical curves
x:	The first waypoint of the atom position in the crystal lattice
X:	Anion
y:	The second waypoint of the atom position in the crystal lattice
$y_{i\ calc}$:	The calculated intensity
$y_{i\ obs}$:	The observed intensity
z:	The third waypoint of the atom position in the crystal lattice
Z:	The atomic number

Greek letters

χ^2:	The agreement factor
λ:	Wavelength of the X-rays
θ:	Bragg diffraction angle[°]
ϑ:	The Frequency(s^{-1})

Subscripts and Superscripts(Indications)

Cub: It means that the crystal direction is in the cubic structure

hkl: Miller signs

n: oxidation number

m: oxidation number

Abbreviations

APF:	Atomic Packing Factor
ASTM:	American Society for Testing Materials
CCD:	Charge-Coupled Device
EDS:	Energy Dispersive X-ray spectroscopy
GHG:	Greenhouse Gas
GoF:	Goodness-of-Fit
SEM:	Scanning Electron Microscope
SOFC:	Solid Oxide Fuel Cell
XRD:	X-Ray Diffraction

General introduction

General introduction

Energy is one of the most important topics which attracted the attention of researchers, and enjoyed their interests from everlasting because the multiplicity of its used fields that the global demand growth about it increase as a result of the industrial progress and the fast population growth, with the knowledge increasing of the threats which facing the Earth's environment by the use of conventional energy, which can be identified in the fossil fuel(gas, petroleum…) and the nuclear energy, this produces a number of problems which is conversant with the individual and environmental at the same time, and the exploitation of traditional energy sources in factories; homes and transportation cause air pollution by the toxic gases**[1]**.

CO_2 is the main gas responsible for the greenhouse effect (53% GHG), it is important to focus on the CO_2 emission to be able to reduce or even compensate.

Energy sources are classified into three different categories: Fossil fuels that come from the combustion of natural reserves, which were formed over millions of years from organic deposits (plants or tiny animals); Nuclear energy (Atomic), which comes from the energy that binds the particles of atomic nuclei between them and it is taken from a radioactive mineral: Uranium and the third class is the renewable energy which is produced from renewable natural sources**[2]**.

From among these renewable energies, scientists have tried to exploit all of the wind power; solar energy; water energy... etc. But all these alternative sources suffer from some drawbacks which make them a limited applications, they are very expensive and are subject to the vagaries of the atmospheric climate, in addition to the storage problems. The thing that prompted the researchers to go to another alternative source, is the hydrogen where these researchers reach to make compounds based on hydrogen as a fuel to her, the so-called fuel cell which operated efficiency up to about 60%. So its types and shapes are multiplied depending on the material of which makes electrolyte.

Fuel cells are considered the most technical and successful types of renewable energy sources due to the use of hydrogen and oxygen who passing by a large proportion in the nature. In addition to maintaining the environment integrity and this is reflected in the lack of toxic gases sent as the first and second carbon oxide(CO, CO_2), and the most important of these types is the solid oxide fuel cell(SOFC) which is characterized by high efficiency in energy production, as an estimated 70%. However, the biggest disadvantage is the high degree of operating temperatures which up to 1000 °C and this is what leads to the length of the take-off, for this

reason, it requires the use of expensive price materials for their manufacture as the porcelain, and to address this confusion will reduce the cost of cells and ensures its reliability over the long term.

All these reasons have made researchers are searching in the manufacture material of electrolyte which has a structure with porous nature and high ionic conductivity at the moderate temperatures. These is credited to the rapid and enormous progress which witnessed the physics of solids interested with studying the crystalline materials in terms of their virtual shape and their internal composition, and that by the use of characterization techniques that avoid the material damaging and the waste of time as the detecting with X-rays that have been discovered by the world William Conrad Roentgen in 1895, where the latter has opened a broad prospects to get to know most of the crystal structures of materials and therefore to predict its physical and chemicals characteristics**[3, 4]**.

Among the oxides which show ionic conductivity for oxygen at moderate temperatures, the brownmillerite compounds $Ca_{1-x}Sr_xFeO_{2.5}$ that falling from the perovskite structure, where it was the study of oxygen diffusion mechanism for the $Ca_2Fe_2O_5$ compound at room temperature by x-ray diffraction and found that it contains channels are likely to pass through ions which are formed by the convergence of octahedral surfaces models (FeO_6) with tetrahedral surfaces Models (FeO_4). It should also be noted that this mechanism also occur in the $Sr_2Fe_2O_5$compound**[5]**.

So, our aim from this work is to find a mathematical model that calculates the oxygen rate in the $Ca_{1-x}Sr_xFeO_{2.5+y}$ compounds (x=0.5; 0.7; 0.90) using its lattice parameters which are extracted from the Fullprof program by the "le bail" refinement method.

This work is structured in the form that allows to read it at various levels, and it contains three chapters:

Chapter I: addresses an overview of the brownmillerite structure. Beginning with perovskite structure, its types followed by the tolerance factor and the physical properties, and then pass to the brownmillerite structure and ionic conductivity, we conclude with studying the $AFeO_{2.5}$(A=Ca, Sr) compounds which belong to the series of $Ca_{1-x}Sr_xFeO_{2.5}$ compounds.

Chapter II: we describe the characterization techniques beginning of the x-ray diffraction: its definition; production and the experimental methods of its diffraction, then we studying the EDS technique coupled to SEM.

Chapter III: we use FULLPROF software for the determination of lattice parameters related to the $Ca_{1-x}Sr_xFeO_{2.5+y}$ compounds(x=0.5, 0.7, 0.9), then we will use these results to achieve a mathematical model for Calculation of oxygen rate in the series of $Ca_{1-x}Sr_xFeO_{2.5+y}$ compounds.

Finally, we conclude this work with a general conclusion which collects the different studied aspects.

Chapter I

$AFeO_{2.5}$ compounds (A=Ca, Sr)

I. $AFeO_{2.5}$(A=Ca, Sr) compounds:

Introduction:

Fuel cells are one of the best renewable energy technologies that serve the technology in the modern time. As it is called in this day a source of energy twenty-first century, it has been a very important interest by experts and researchers where there were many kinds and shapes; including with electrolytes solid oxide fuel cells (SOFC), which is considered one of the finest efficiency cells in the production of energy.

Since the invention of the fuel cell of the type SOFC, scientists hope to get to the making of high-efficiency cells working with materials be operated degree temperature at the room temperature, and was the last of these used compounds brownmillerite emanating from perovskite family, and this structure can operate at low temperatures, In addition, it is characterized by high ionic conductivity and weak electronic.

From this point it will be addressed in this chapter to structure of $Ca_2FeO_{2.5}$ and $Sr_2Fe_2O_{2.5}$ compounds after giving an overview of the perovskite and brownmillerite structure, also on ionic conductivity.

I.1 An overview of the brownmillerite structure:

I.1.1 The perovskite structure:

The structural family of perovskites is a large family of compounds having crystal structures related to the mineral perovskite $CaTiO_3$. The mineral was discovered from samples found in the Ural mountains(Russia) by Gustav Rose in 1839, and after that it was named by the Russian mineralogist L. A. Perovski(1792-1856)**[6]**.

The perovskite crystal structure was published for the first time in 1945 from X-ray diffraction data on barium titanate by the Irish crystallographer H. D. Megaw (1907-2002). It is a true engineering ceramic material with a plethora of applications spanning energy production(SOFC technology), environmental containment and communications.

The general stoichiometry of the perovskite structure is ABX_3, where A and B are cations in the original perovskite mineral ($CaTiO_3$). the A cation is divalent and the B cation is tetravalent. $CaTiO_3$ exhibits an orthorhombic structure in space group *Pnma*. and X is an anion(O^{2-}, S^{2-}, F^-, Cl^- et Br^-) together form a close-packed array, comprising AX and X_2 rows(Fig. I-1)**[7]**.

The B cations are located in octahedral that have arisen of adjacent layers X anions. This structural family is important in terms of compositional diversity and abundance. It is estimated that more than 50% of the terrestrial volume is composed of perovskites minerals**[6,8]**.

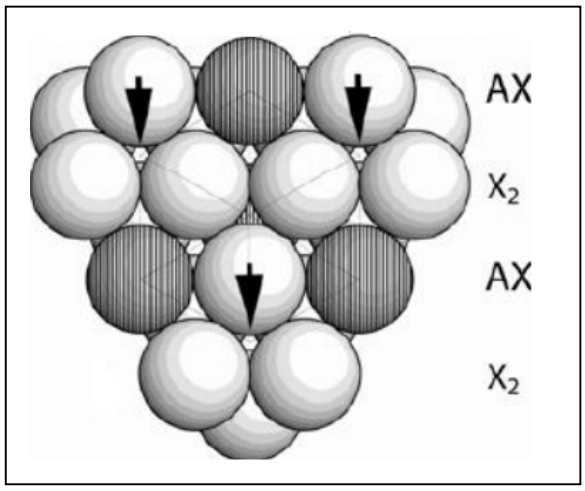

Figure (I.1): The perovskite structure with close packed arrays **[4]**.

I.1.1.1 Structural description:

The general formula of perovskite is ABO_3.In the ideal case, perovskite characterized with cubic structure in space group Pm-3m and is susceptible to accommodate almost all of the elements in the Mendeleïev periodic system for the sites A and B where A^{n+} is an alkali metal, alkaline earth or a rare earth element, and B^{m+} a cation from the family of transition metals.

To form an oxide with a perovskite structure, a couple (A^{n+}, B^{m+}) given must meet a number of specifications. On the one hand, the sum of the oxidation numbers n and m of the cations must equal 6 for the charge of the compound is generally null, on the other hand, ions of the congestion in the structure requires that the ionic radii of the cations are consistent with the geometry of the perovskite lattice.

The cation of smaller size (B^{m+}) is placed on top of a cube with the O^{2-} anions occupying the center of the edges and the cation A^{n+} the center of the cube. The coordination numbers of O^{2-} and B^{m+} ions are 6 while the cation A^{n+} is placed in the cavity in coordinated cubo octahedral 12.

There are generally two types perovskites following the occupation of the A and B sites:

- **Simple perovskite structure:**
  In this case, The A and B cations are occupied with one type of atoms($BaTiO_3$, $PbTiO_3$, $CaTiO_3$, ….)
- **Complex perovskite structure:**
  In this type from the structural composition that A or B are occupied with two types of atoms as: $PbSc_{1/2}Ta_{1/2}O_3$, $Na_{1/2}Bi_{1/2}TiO_3$,… **[6,8]**.

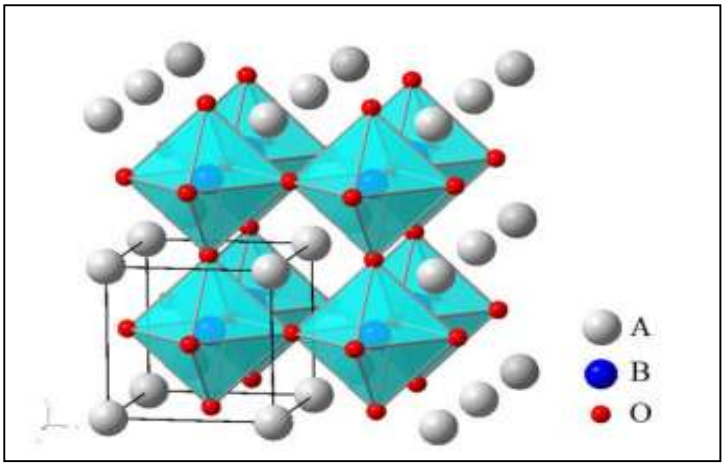

Figure (I.2): The perovskite structure ABO_3**[3]**.

I.1.1.2 Tolerance factor:

To understand and studying perovskite's structure, Goldschmidt define a dimensional quantity called tolerance factor (Factor of Goldschmidt, the founder of the science of crystal chemistry).

$$t=\frac{(r_A+r_O)}{\sqrt{2}(r_B+r_O)} \qquad (I.1)$$

where r_A , r_B and r_O are the ionic radii of A^{m+}, B^{n+} and O^{2-} respectively**[9]**.

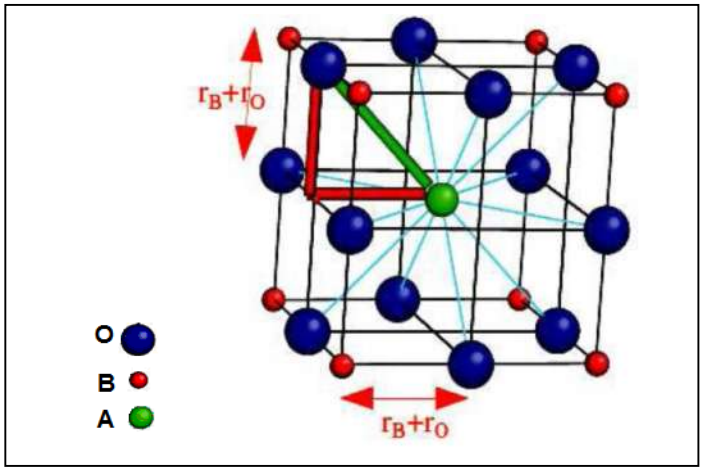

Figure (I.3): Dimension of cubic perovskite cell**[9]**.

In the ideal case, the perovskite structure crystallizes in the cubic system with space group $Pm\bar{3}m$. (This is the case for $SrTiO_3$). Sr^{2+} and O^{2-} ions have approximately the same radius ($r(Sr^{2+})$=1.44 A°, $r(O^{2-})$=1.40 A°), and Ti^{+4} fits into the octahedral site($r(Ti^{4+})$=0.61 A°, ($\sqrt{2}$-1)*$r(O^{2-})$=0.58 A°)**[8]**.

In general, this cubic cell undergoes deformations and a decrease of the crystal symmetry for lower values of t, this could give an idea of the formation of a perovskite structure of non-idea kind (Table. I-1).

Table (I.1): Distortions of perovskite structure according to the values of t**[9]**.

t<0.75 ilmenite	0.75<t<1.06 perovskite			t>1.06 hexagonal
	0.75<t<0.95 orthorhombic distortion	0.96<t<0.99 rhomboedric distortion	0.99<t<1.06 cubic	

I.1.1.3 Physical properties of perovskite:

Probably because of the abundance of oxygen, much scientific work has been focused on perovskite oxides. Of general importance for this class of compounds is the chemistry of the BO_6 octahedra. In most compounds, the A^{m+} ion will not contributing to electron states that govern the transport or magnetic properties. For example, the conduction properties can be explained by examining the electronic configuration of the B^{n+} ion. Thus, $SrTiO_3$ with Ti^{4+} ions (d^0) is an insulator since it does not have any electrons in the conduction band, in contrast to $LaNiO_3$ (Ni^{3+}, d^7) and $LaCuO_3$ (Cu^{3+}, d^8).

However, Sharma and others showed that $LaNiO_3$ becomes less metallic when going from Ln = La to Pr, Nd and Sm, due to the lanthanide contraction that will lead to a wider band gap.

Important materials with perovskite or perovskite-related structures, possessing interesting properties can be found in table(I-2).

Table (I.2): Physical properties for some perovskite's compounds**[10]**.

Compound	**Physical property**	**Application**
$CaTiO_3$	Dielectric	Microwave
$BaTiO_3$	Ferroelectric	Non-volatile computer memories
$PbZr_{1-x}Ti_xO_3$	Piezoelectric	Sensors

$Ba_{1-x}La_xTiO_3$	Semiconductor	Semiconductor
$Y_{0.33}Ba_{0.67}CuO_{3-\delta}$	Superconductor	detectors of magnetic signals
(Ln, Sr)$CoO_{3-\delta}$	mixed ionic and electronic conductor	Gas diffusion membranes
$BaInO_{2.5}$	ionic conductor	Electrolyte in solid fuel cells
$AMnO_{3-\delta}$	giant magnetoresistance	Read heads for hard disks

Oxygen ion conduction is an important property in applications such as fuel cells and oxygen-permeable membranes. Generally, in traditionally used materials for fast oxygen conduction, temperatures near 1000˚C are needed. Research is being done to obtain materials that can be operated at lower temperatures, since this would facilitate the operation of the applications.

In 1986 it was discovered that some perovskite-related cuprates become superconductors at higher temperatures that had been obtained for any other materials. This finding boosted the science in the whole field of perovskite-related oxides. The example compound in table(I-2), La2-xBaxCuO4 was the first so-called high-temperature superconductor found. This discovery has reinforced science in the whole field of type oxides perovskite-related. As can be seen, scientific research deviates from the ideal type ABO_3 to their derivatives**[8,10]**.

I.1.1.4 Perovskite-related:

The Perovskite structure elasticity, in addition to the Non stoichiometry result in many phases as shown in Figure(I-4), When adding AO to Perovskite structure transformed into a phase A_2BO_4(Ruddledsen-Popper). But when adding BO_2 produces AB_2O_5 phase As an example Pseudobrookite, And the phases that can be obtained from the change of oxygen content through the oxidation and reduction process respectively are $A_2B_2O_7$(Examples include Pyrochlore oxides), and $A_2B_2O_5$ which called Brownmillerite.

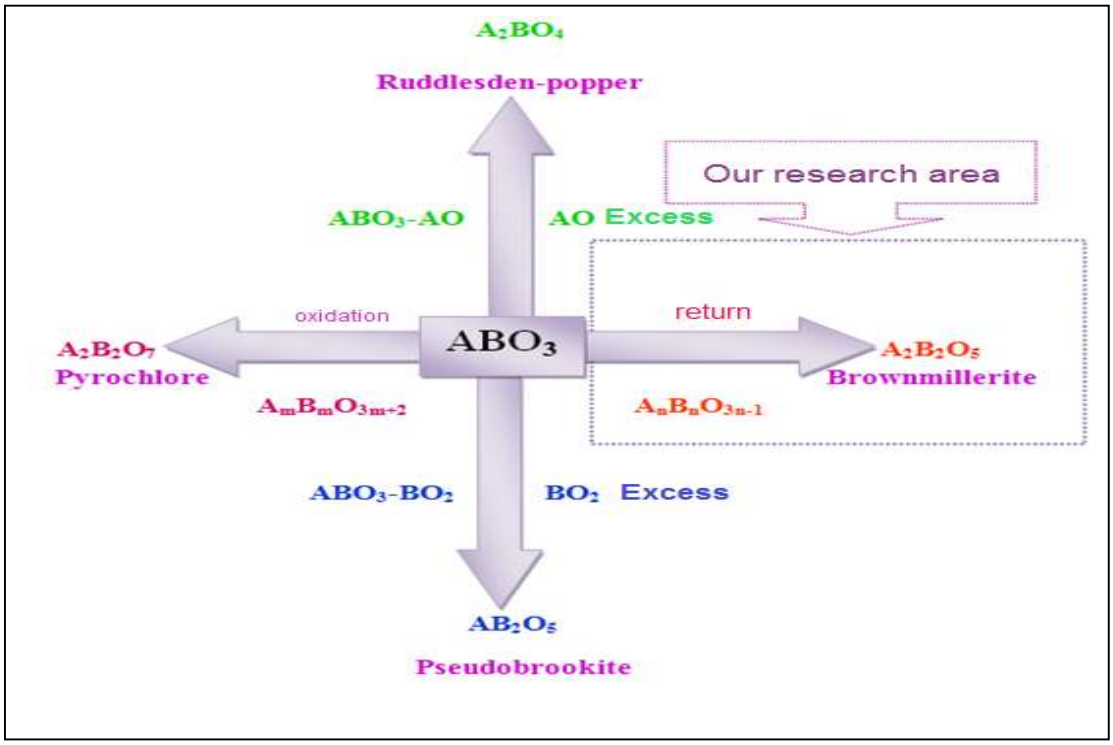

Figure (I.4): The derivatives of Perovskite structure**[3]**.

To illustrate more that the intended $ABO_{2.5}$ phase deducted from ABO_3 by introducing oxygen vacancies in the $[110]_{cub}$(And cub symbol indicates that the crystalline direction is in cubic structure), (Figure. I-5)**[3,6,8,11]**.

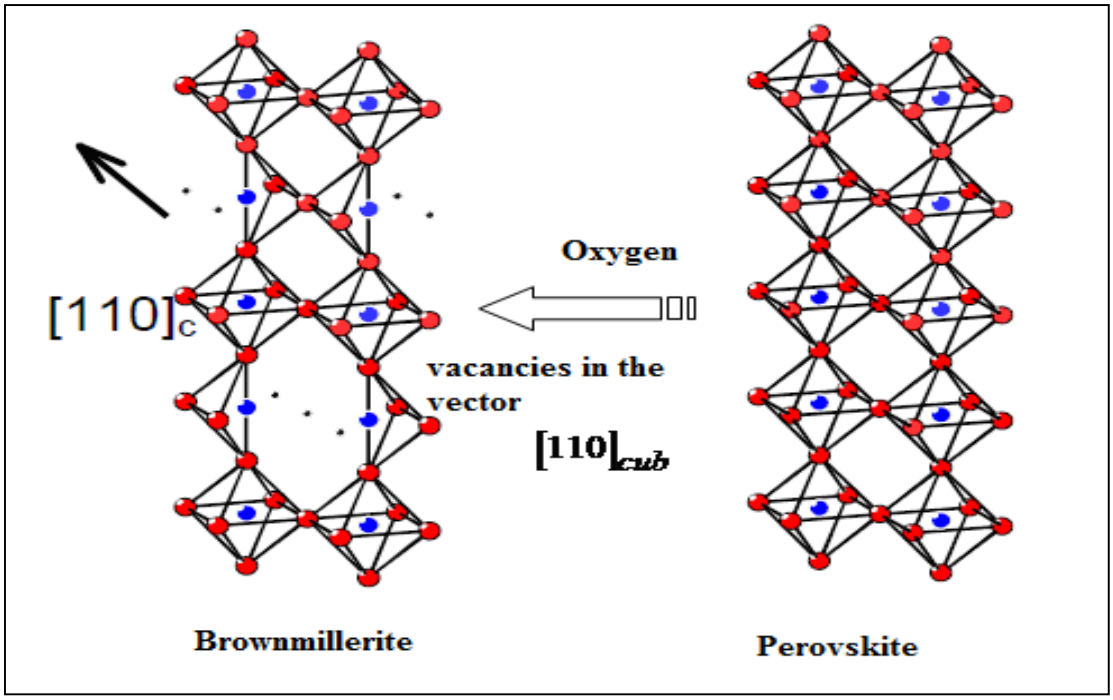

Figure (I.5): Derivation of brownmillerite structure by the presence of oxygen vacancies in the vector $[110]_{Cub}$ of Perovskite structure**[6]**.

I.1.2 The brownmillerite structure:

Brownmillerite structure called according to the scientist brownmiller, who discovered it in 1928 accompanied by Hansen when they made the first study on the following compound:Fe_2O_3, CaO, Al_2O_3.

The brownmillerite structure $A_2B_2O_5$(or $ABO_{2.5}$) with its alternating layers of corner sharing octahedral BO_6(O) and tetrahedral BO_4(T) along the b axis (see figure. I-6) has a unit cell related to the basic perovskite cell by: $a \approx c \approx \sqrt{2} * a_p$, $b \approx 4a_p$(where a_p denotes the unit-cell edge of the perovskite subcell).

A structural model for $A_2B_2O_5$ can be derived from the perovskite structure ABO_3 by removing one-third of the oxygen ions in every other (0k0) layer of octahedra in rows that are parallel to the c axis (a<c< b). These gaps that form one-dimensional migration routes for the diffusion of ions in the tetrahedral layers can contribute significantly to oxygen ion transport**[8,4,11,12,13]**.

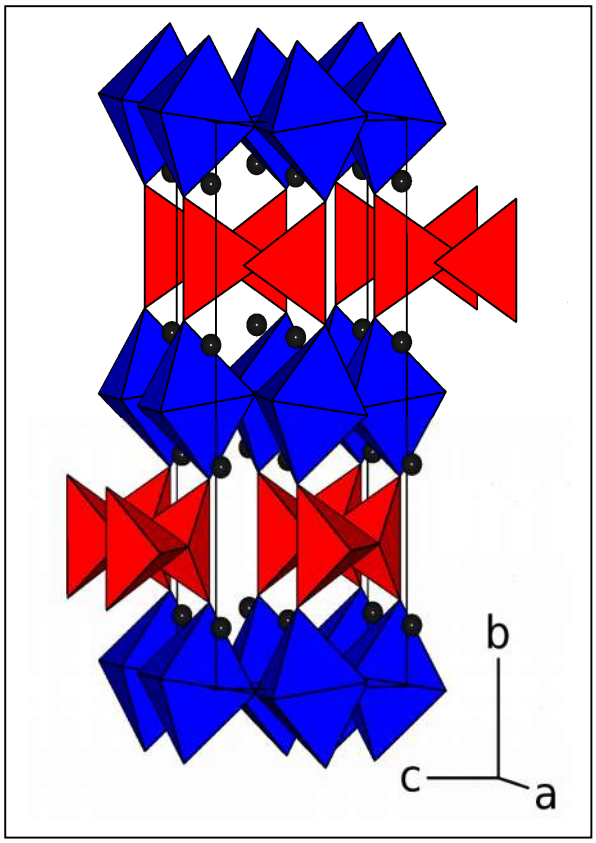

Figure (I.6): Brownmillerite structure $ABO_{2.5}$**[5]**.

The scientific research in crystallography science showed that these compounds crystallize in space group *Imma*, but the first real studies by x-ray diffraction that achieved by the scientist Bertaut on single crystal received ambiguous in finding structural solutions, and the use of statistical method proved to be the condition h+k+l=2n+1 that belong to the bravais lattice of the

type P and space group *Pnma*. On the other hand, it has made structural studies of similar compounds $SrFeO_{2.5}$, $Sr(Fe,Co)O_{2.5}$, $CaFeO_{2.5}$, $SrMn_{0.5}Ga_{0.5}O_{2.5}$, $BaInO_{2.5}$ which have been studied by neutron diffraction because it is the most sensitive technique for oxygen atoms and give more accurate description for alternating the tetrahedral BO_4 and all this research has shown that brownmillerite phases can crystallize in the space group *Imma*, *Pnma* and *I2mb* as shown in figure(I-7)**[3,11]**.

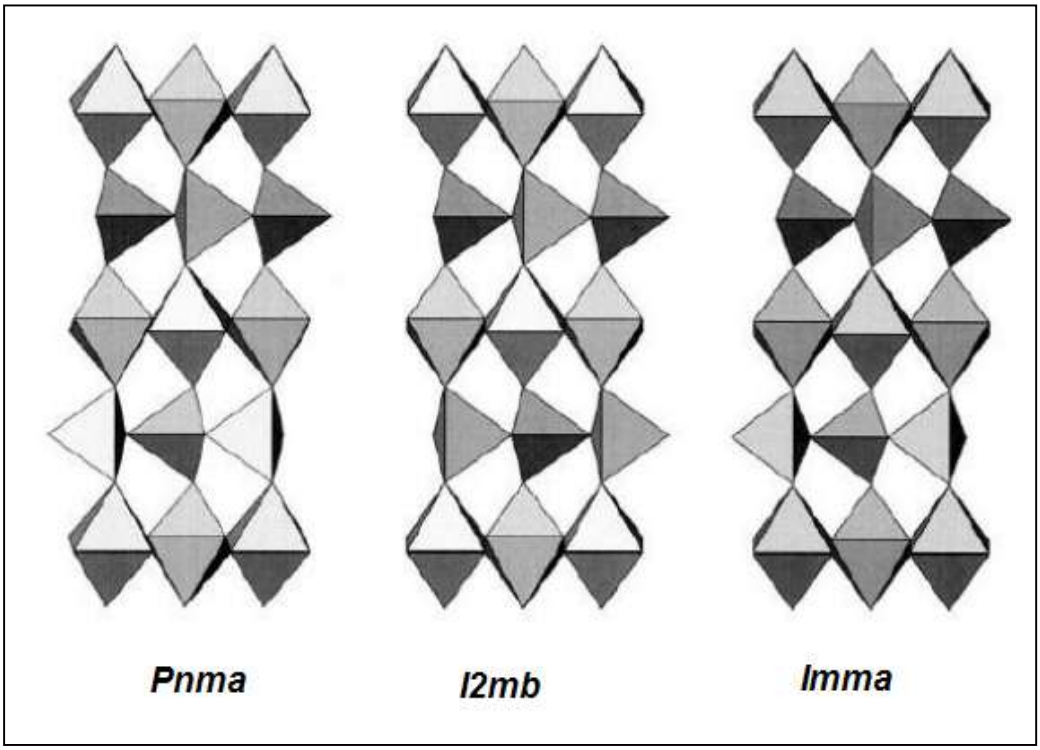

Figure (I.7): Possible space group of brownmillerite**[12]**.

I.2 Ionic conductivity:

The decrease of oxygen in the perovskite structure, allows the creation of vacancies to enable the transfer of ions (anions or cations) across it from one place to another(see figure. I-8). The ionic conductivity is considered a functional element underpinning solid oxide fuel cells compounds (SOFC) in electrical energy production process.

In recent years, the researchers prepare new material of good conductivity for oxygen ions from brownmillerite category known oxide high conductivity of ions through the application of private standards. For example, $Ba_2In_2O_5$, $Sr_2Sc_{1.3}Al_{0.7}O_5$ which owns conductivity 55.10^{-3} Scm^{-1}, 1.10^{-3} Scm^{-1} respectively at a temperature of 700 °C**[4,6]**.

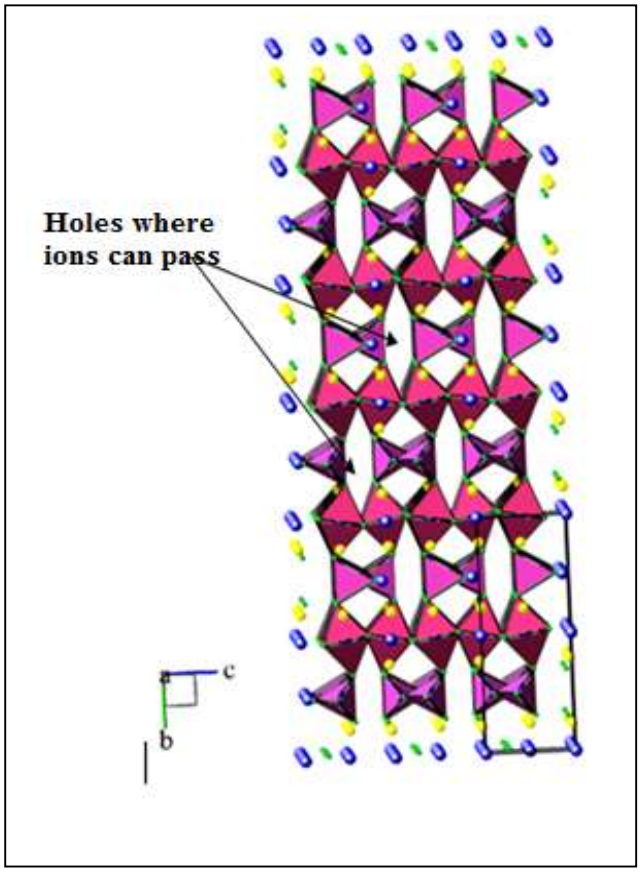

Figure (I.8): Illustration places to cross the oxygen ions**[3]**.

I.3 (Ca, Sr)$FeO_{2.5}$ system:

I.3.1 $Sr_2Fe_2O_5$ Structure:

The $Sr_2Fe_2O_5$ structure belongs to the type of brownmillerite structures. It consists of alternating layers bound by the peaks of tetrahedra FeO_4 and octahedra FeO_6, where the order of the oxygen vacancies thus creates octahedra layers shared by summits (denoted O) alternating with tetrahedral layers shared by summits (denoted T) stacked in an order OTOTOT ... …, as shown in Figure. I-9. In this structure (which takes the name of the mineral brownmillerite Ca_2FeAlO_5), half of Fe cations are in octahedral sites and half in the tetrahedral sites.

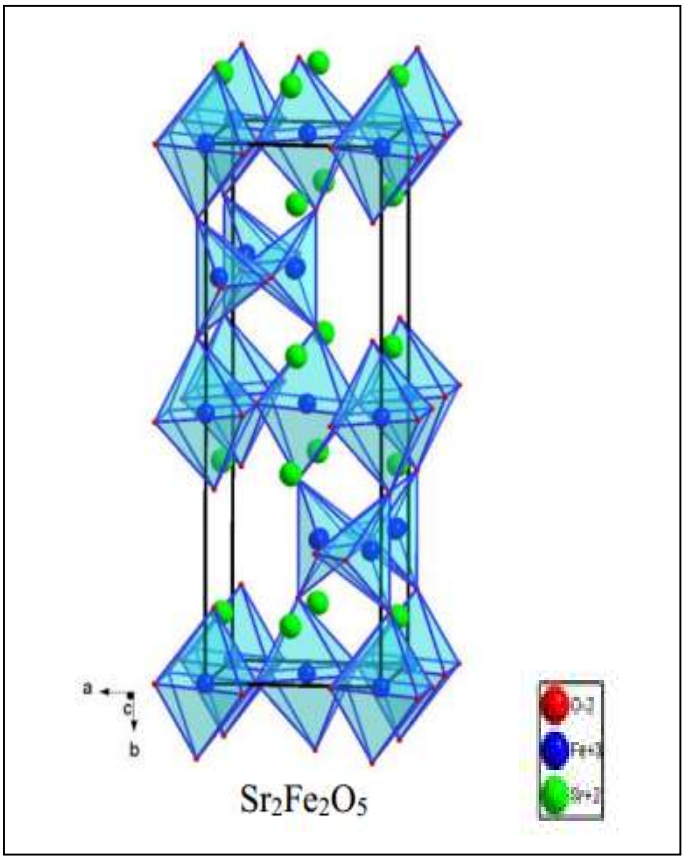

Figure (I.9): The $Sr_2Fe_2O_5$ model **[8]**.

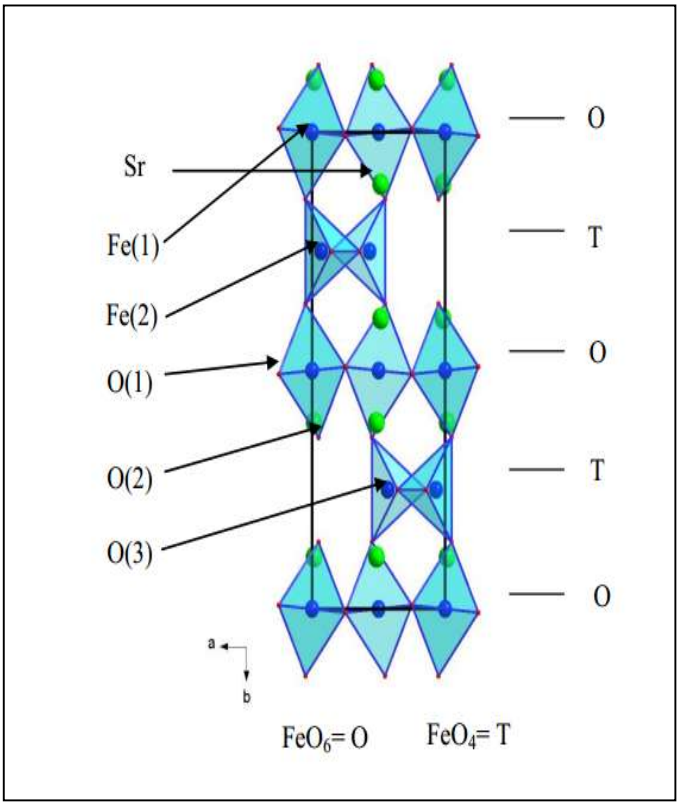

Figure (I.10): $Sr_2Fe_2O_5$ Structure showing the layers of alternate octahedra with tetrahedra FeO_4**[8]**.

The next table present atom positions in $Sr_2Fe_2O_5$ compound .

Table (I.3): The atom positions in $Sr_2Fe_2O_5$ compound **[12]**.

Atom	X	y	z
Sr	0.0159	0.10933	0.5
Fe(1)	0	0	0
Fe(2)	-0.0678	0.25	-0.0445
O(1)	0.25	-0.0077	0.25
O(2)	0.0490	0.1402	0
O(3)	-0.1421	0.75	0.6245

The results of powder neutron and monocrystal X-ray diffraction shows that $Sr_2Fe_2O_5$ has a structure disordered *Imma*, or ordered *I2mb* with one type of tetrahedral chains.

The description of the $Sr_2Fe_2O_5$ structure in both space groups *Pnma* and *I2mb* differ only by the symmetry of the octahedral site of the cation. So, we observe different orientations of tetrahedrons along the b axis, this means that alternating order OTOT' in *Pnma* and *Imma*, and an order of OTOT in *I2mb*, the latter having been observed in a study of a simple monocrystal of $Sr_2Fe_2O_5$.

The lattice parameters of $Sr_2Fe_2O_5$ structure are: ***a***= 5.5253 Å, ***b***= 15.5775 Å, and ***c***= 5.6688 Å.

No increase in the ionic conductivity is found after a similar first order transition in the structure isomorphous $Sr_2Fe_2O_5$ at 700 ° C, suggesting an ordered arrangement of oxygen vacancies above 700° C, while rest $Ca_2Fe_2O_5$ steady until at least 1100 ° C.

Examination of $Sr_2Fe_2O_5$ Mössbauer spectroscopy showed that the tetrahedral coordination Fe persists even in the apparent disordered material. It was therefore proposed that the order breaks into microdomains of a size not discernable by XRD measurements**[8,11]**.

I.3.2 $Ca_2Fe_2O_5$ Structure:

The bicalcite ferrite $Ca_2Fe_2O_5$ is a compound that also belongs to the brownmillerite family $A_2B_2O_5$. Several research has been devoted to the examination of $Ca_2Fe_2O_5$ brownmillerite

compounds which crystallize in the orthorhombic system with space group *Pnma* and the following lattice parameters:

a=5.4253 Å, ***b***=14.7687 Å, and ***c***=5.598 Å.

The $Ca_2Fe_2O_5$ structure is obtained in the cubic perovskite by removing a third oxygen ion in each layer of octahedral parallel to the axes $[110]_c$. It is built of alternating layers along the b axis tetrahedra and twisted octahedra bound by summits(Fig. I-11).

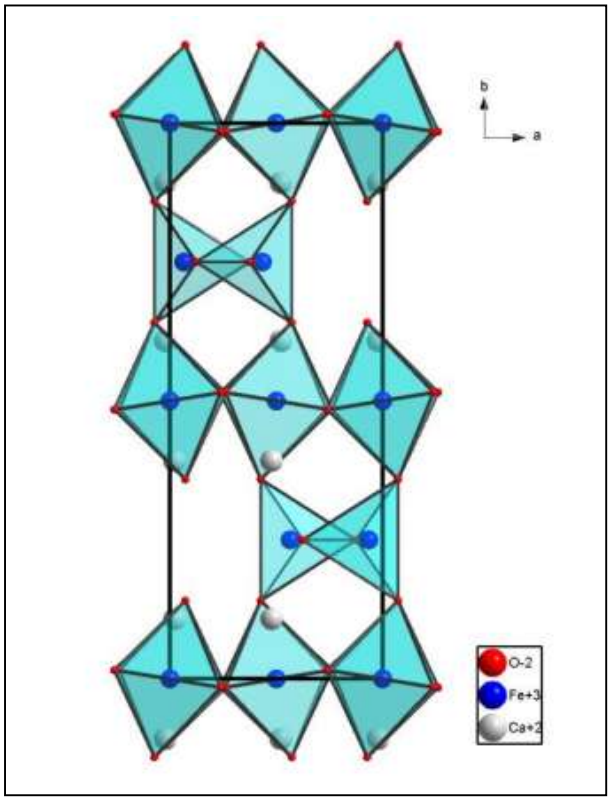

Figure (I.11): $Ca_2Fe_2O_5$ Structure **[8]**.

Atomic positions found by Berastegui et al shown in the Table(I-4)**[12]**.

Table (I.4): Fractional atomic positions in the compound $Ca_2Fe_2O_5$**[12]**.

Atom	x	y	z
Ca	0.0221	0.1078	0.4826
Fe(1)	0	0	0
Fe(2)	-0.0656	0.25	-0.0543
O(1)	0.2382	-0.0156	0.2634
O(2)	0.0727	0.1408	0.0236

O(3)	-0.1246	0.25	0.5994

Berastegui et al found after their structural study on $Ca_2Fe_2O_5$ compound depending on the temperature where the lattice parameters vary linearly with temperature while a structural phase transition from *Pnma* to *Imma* occurs at 700 °C. This transition induces a change in the tilt of octahedra and the movement of oxygen ions in tetrahedra which construct a form of alternative layer structure.

In addition, the continuous change of the lattice parameters (Fig. I-12) suggests a second order phase transition. Thus, it is possible at 700 ° C the two symmetries can be observed. However, the broad reflections observed at higher interatomic distance values may suggest that there is an order to short-range areas with an order type of oxygen vacancies can be described by *I2mb*. It may be noted that in $Sr_2Fe_2O_5$ octahedra are more twisted than $Ca_2Fe_2O_5$, while the reverse is true for tetrahedral**[8]**.

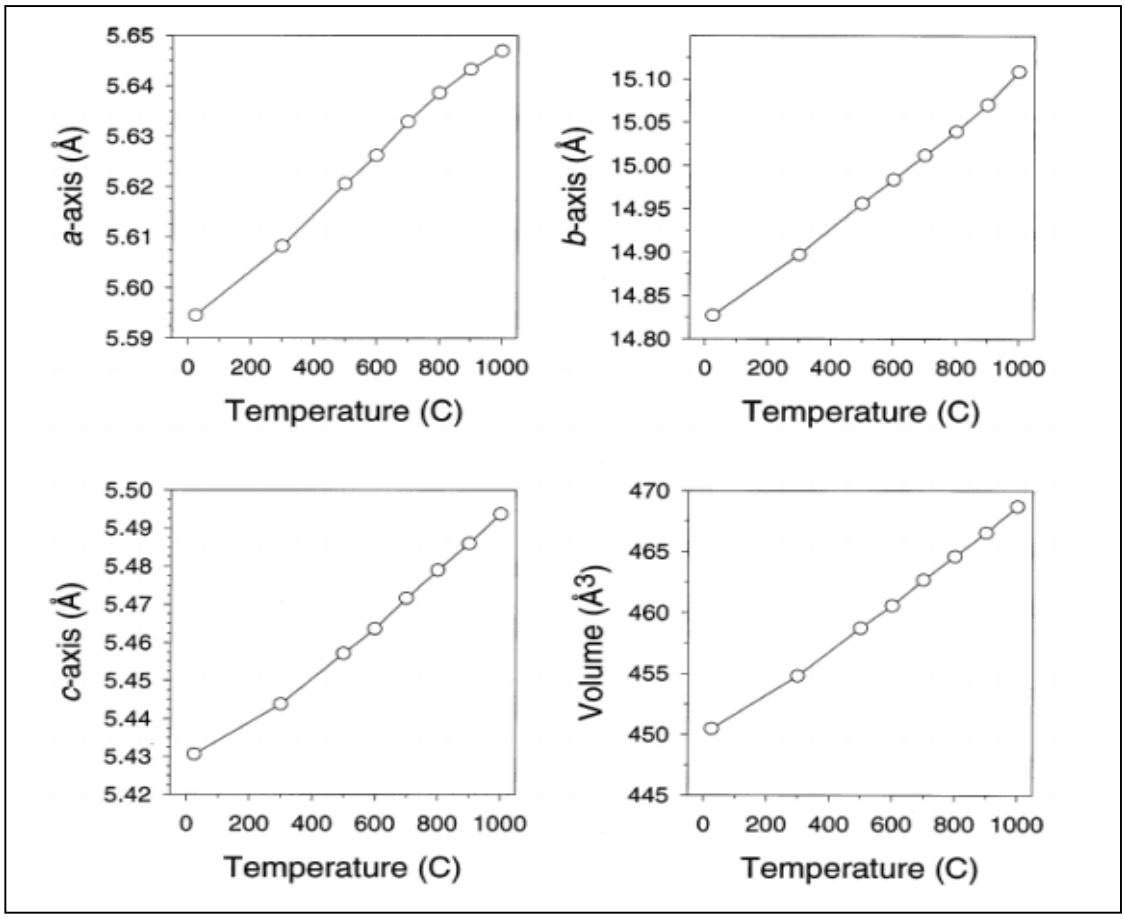

Figure (I.12): Change in the lattice parameters depending on the temperature in $Ca_2Fe_2O_5$**[12]**.

Conclusion :

Our study was based in this chapter to identify the (Sr, Ca)$FeO_{2.5}$ system that belongs to the brownmillerite family which allows good ionic conductivity and are derived from the crystalline oxides family(perovskite), as we highlighted on the physical properties of these compounds which can be obtained by characterization techniques that will be studied in the next chapter.

Chapter II

Characterization techniques

II. Characterization techniques:

Introduction:

In this chapter, different analyzes were performed using complementary techniques with a view to understand the influence of the synthesis method of the crystallographic structure of the compounds studied in this work. The characterization techniques are presented in the following order: the X-ray diffraction and Energy dispersive spectroscopy (EDS) coupled to SEM.

II.1 X-ray diffraction:

II.1.1 Nature of X-rays:

X-rays are essentially electromagnetic waves flow between the scope runs between gamma rays (high energy) and ultraviolet (minimum energy) and therefore, they are invisible rays with great frequency and small wavelength and expressed by angstrom (Å), range between 0.1 and 100 Å. These limits are not precise so they vary depending on the method of their production which is equivalent to an energy field from 1 to 100 Kev**[4,14]**.

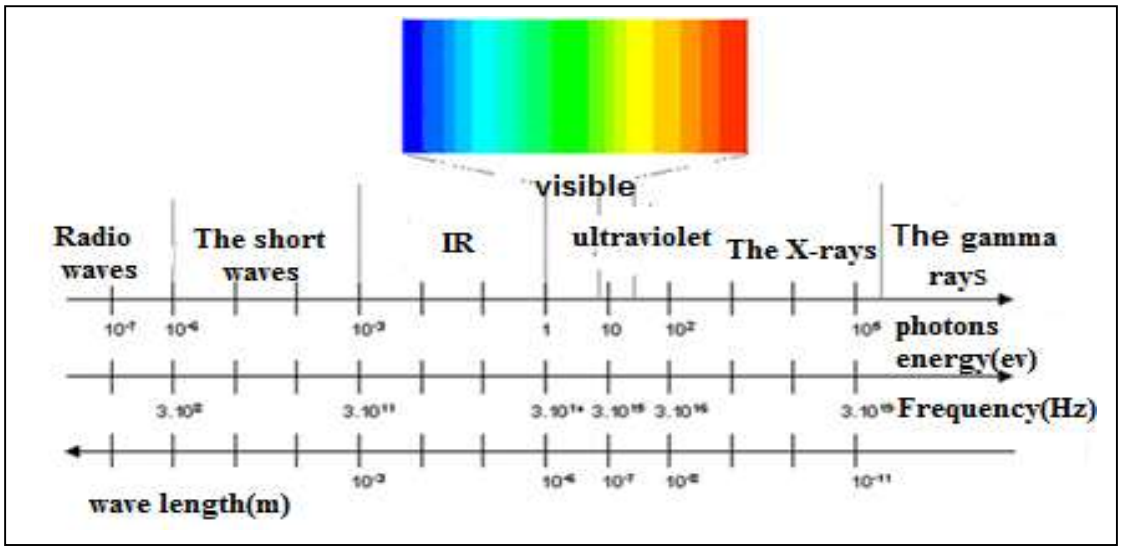

Figure (II.1): X-ray position in the electromagnetic spectrum**[15]**.

It has a dual nature as the rest of the electromagnetic radiation(wave-particle) can be described at a wavelength λ or with the photon energy E(photon is a null mass and charge particle and moves with the light speed C). The energy is given by:

$$E = h\vartheta = \frac{hC}{\lambda} \qquad \text{(II-1)}$$

Where: C=3.10^{8} m/s, *h*=6.62.10^{-34} J.s(Planck constant).

By compensation in the previous relation, we find:

$$E=\frac{12398}{\lambda(\text{Å})} \qquad \text{(II-2)}$$

Where wavelength of the used X-ray in the domain of crystal structure study ranges between 0.5 to 2.5 Å**[14]**.

II.1.2 Production of X-rays:

X-rays generated by the bombing of a particular goal of electrons with energy of 10 to 100 Kev, that producing in the glass tube with a deflated air to avoid this latter interact with electrons, containing two electrodes (cathode and anode), Which form the heart of the production of X-ray device, in addition to a window made of beryllium, which is transparent for X-ray**[5,14]**.

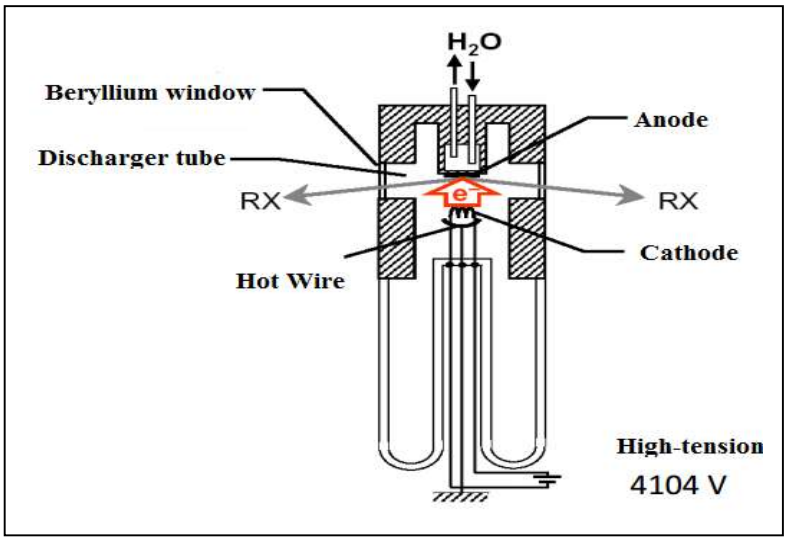

Figure (II.2): Coolidge tube **[16]**.

The idea of the X-rays producing device relies on the electron emissions from the cathode then accelerated under high tension in the direction of the target (the anode), and X-rays emits by the following mechanisms:

- The braking of electrons by the atoms of the target creates a continuous radiation part of which in the field of X-rays.
- The accelerated electrons have enough energy to excite some of the atoms of the target, by disrupting their internal electronic layers. These excited atoms emit X-rays returning to their ground state**[15]**.

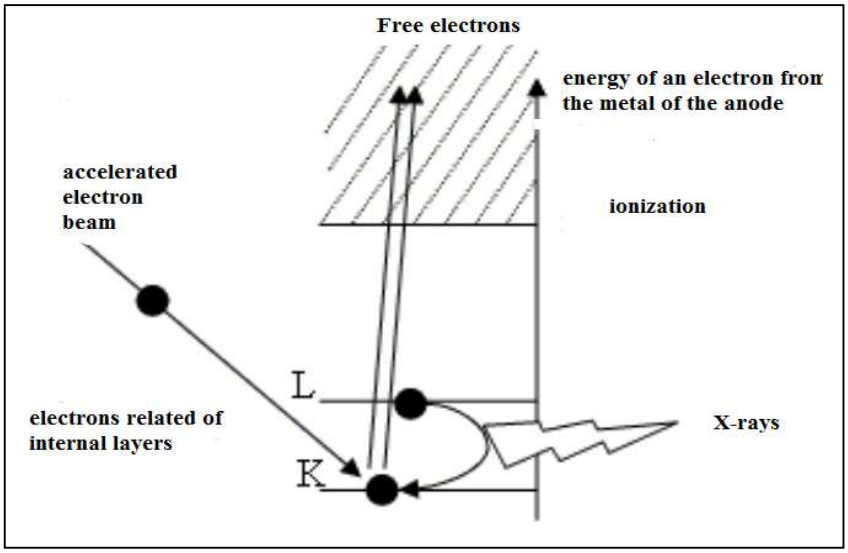

Figure (II.3): Responsible electronic transitions for the generation of X-rays**[15]**.

II.1.3 X-ray diffraction theory:

Diffraction is the waves overlapping phenomenon while it's scattering. the simplest way to study this overlap is by using the diffraction grooved method. In this method we use a sleek of glass wich contains some lines of copper metal where the optical waves can cross through. And "d" is the width distance of the aperture where the ray can enter through, in a condition that the aperture width is equal to the wavelength. So if the overlapping waves are consistent in period, or this difference in period is equal, tow times or three times the wavelength, here we say that the overlap is positive and it gives a bright spot, but if it is negative it gives a dark point**[4]**.

II.1.3.1 The diffraction principle:

Generally, the material is a multi-crystals particle composed of a large number of grains each of which is called mono-crystal, is a regular stacking of atoms, this stacking can be described by a set of crystalline levels of knowledge retinal distances d_{hkl} in terms of Miller signs (hkl), he measured this distance by using X-ray diffraction by Bragg's Law**[14]**.

II.1.3.2 Retinal levels:

The atoms are organized in a crystal on three directions, and called on this organization with crystalline network, the latter can be described as a regular distribution of atoms or molecules or ions, and it is in the form of parallel levels and called the retinal levels. figure (II-4) that explains**[8,14]**.

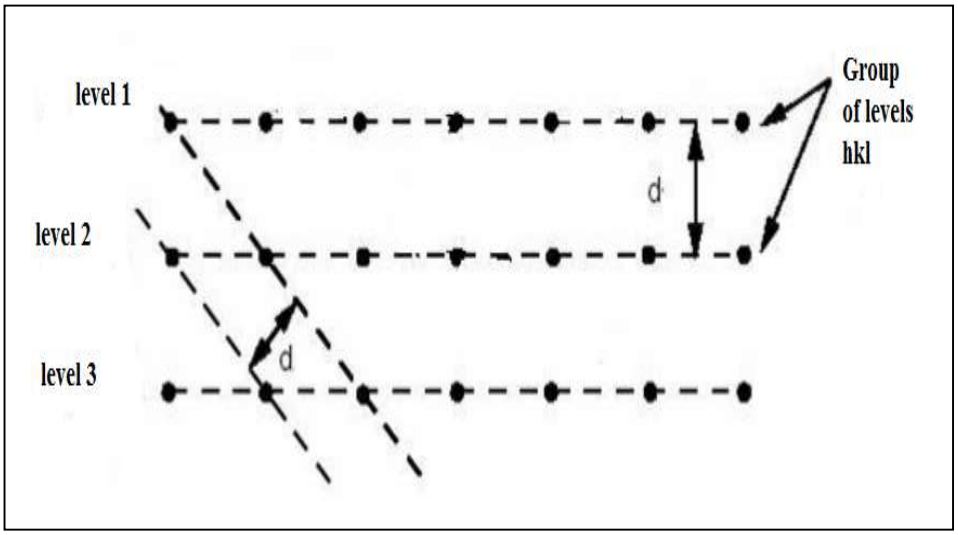

Figure (II.4): A sketch illustrates the retinal levels**[14]**.

II.1.3.3 Bragg's law:

X-ray diffraction method is normally used for structural characterization of the material, allows the identification of the structure of studied material and developed crystallized, it also allows the identification of the size and orientation grains of this material . Its principle depends on the relation of Bragg.

We can explain the process of X-rays diffraction through the model if we think that the single-wavelength beam penetrates the level of atoms or ions, as shown in Figure(II-5)**[14]**.

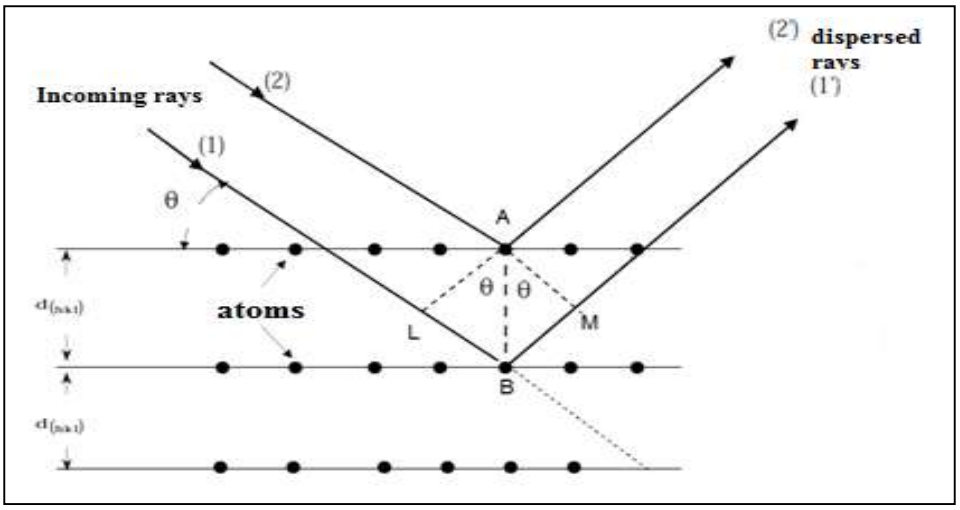

Figure (II.5): Bragg's law**[15]**.

Bragg's law determines certain conditions, occur within them diffraction for packet of radiation on a group of crystalline levels and gives the subject diffractive packet, this law can be expressed in the following relation:

$$2d_{hkl}\sin\theta = n\lambda \qquad \text{(II-3)}$$

Where:

n= reflection order (integer number).

θ= deviation half angle (half of the angle between the incident beam and the direction of the detector).

λ= Wavelength of the X-rays**[17,18,19]**.

II.1.4 The experimental methods of x-ray diffraction:

There are many ways to record the form of x-ray diffraction depends on the form in which the sample if a single crystal or a material in powder form, and also on the type of radiation used that were of a continuous spectrum rays or a single wave rays**[16]**.

II.1.4.1 Single crystal method:

The x-ray diffraction from single crystals is one of the main process ways for appointment the crystal and molecular structure, and include a number of techniques using the crystal rotation and registration the diffraction form by photographic films**[20]**.

- **The Laue method :**

The single crystal sample is fixed and X-rays with different wavelengths are used in this method. Ideally, one would like to use a continuous spectrum of X-rays with various wavelengths that will fulfill the Bragg's law for all sets of planes. However, in reality available wavelengths in X-ray spectral region are limited and, hence, only certain range of d-spacing can be measured. The diffracted X-ray beams are then projected onto a screen of a charge-coupled device (CCD) for all different planes at the same time, whose patterns are thereafter analyzed for determination of the crystal orientation and symmetry as shown in the figure(II.6)**[21]**.

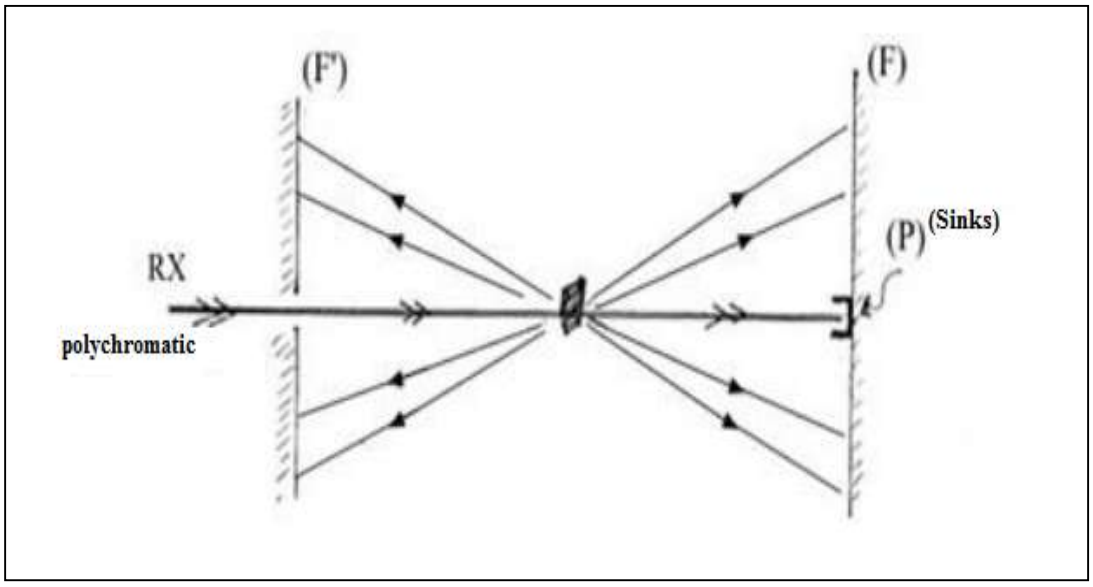

Figure (II.6): Laue method to set the crystal structure**[16]**.

- **The rotary crystal method:**

In the way of the rotary crystal, single wavelength X-rays down on a single-crystal revolves around a fixed axis, and so we get over offline from fall angles θ on the different crystalline levels in the interface distances, and have the opportunity to achieve Bragg law**[3]**.

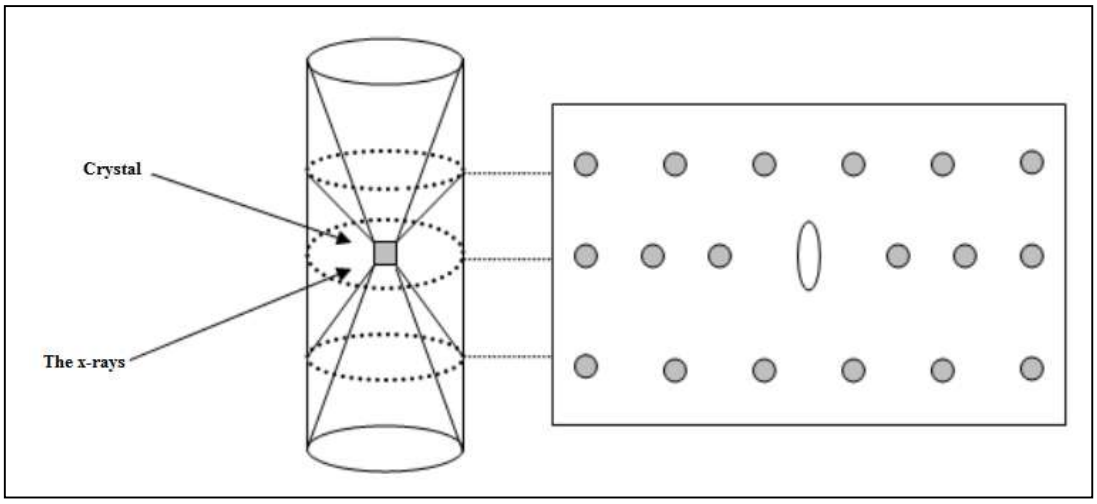

Figure (II.7): Diagram of the rotary crystal method**[22]**.

The figure(II.7) shows a simplified draw for this method. Where the photographic film takes a cylindrical form and its axis is parallels the rotation that the crystal proves about it, And Bragg reflections appear on the delicate film in an horizontal layers**[23]**.

- **The Weissenberg method :**

It also called the moving film method, which is different from the rotary crystal way in the compilation of reflections that are at the same time for only one level of points. We use the cylindrical barriers obscured by all the reflections of the crystal, except which are located on one cone surface, and which are one line on a rotary crystal film, where they spread on the photographic film is placed on a cylindrical carrier moves at a constant speed, parallel to the crystal axis(Figure II.8).

The reflections are grouped on the film during the crystal rotation with an angle 180º and moving the film carrier so that the crystal and film movement is convergent and simultaneous, and on this, all the reflections spread on the whole film surface**[3,16]**.

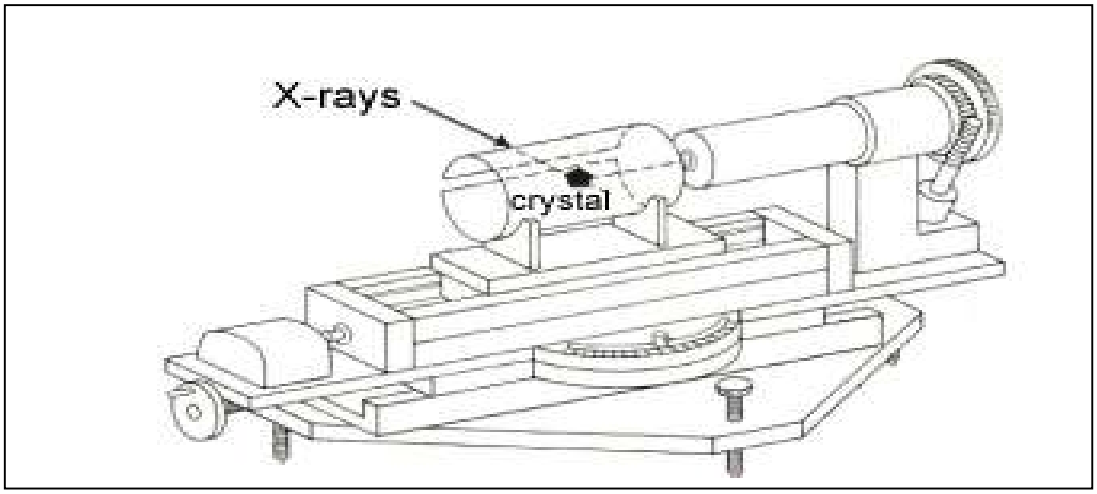

a)Scheme of a Weissenberg camera.

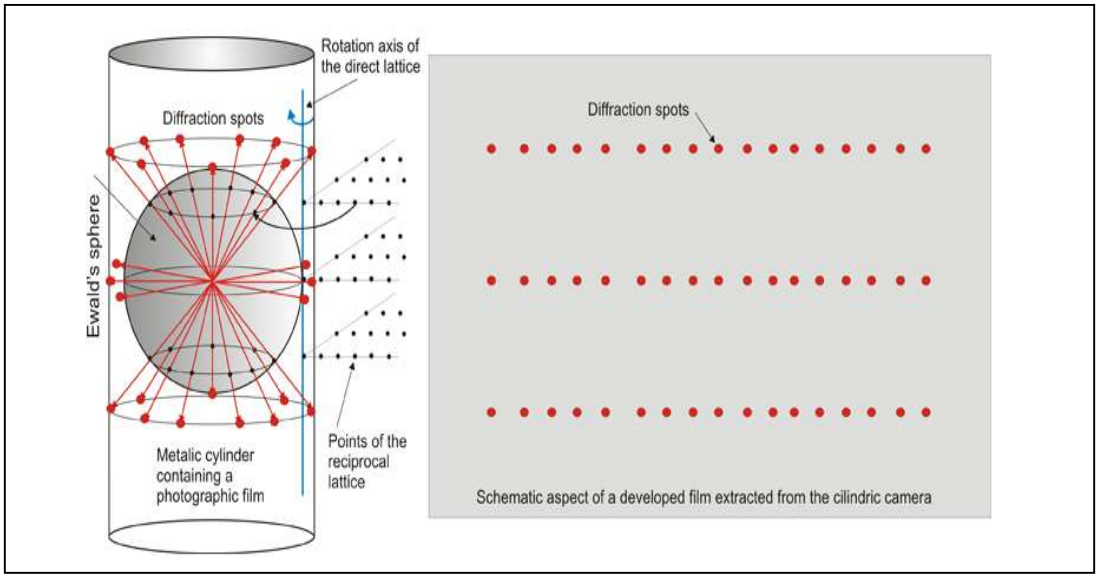

b)Scheme explaining the production of a Weissenberg diagram.

Figure (II.8): a)Scheme of a Weissenberg camera. b)Scheme explaining the production of a Weissenberg diagram**[24]**.

II.1.4.2 X-ray Powder Diffraction:

- **Definition of the powder:**

Some materials are difficult to exist in the form of single crystals and if the amorphous material, but there is in the form of powder, the latter is a small-sized crystals be grains powder, and we get it by grinding material until it becomes the size of grains as little as possible so that we have a sample of the filming of diffraction, where the basic mechanisms used to find a schema known as the first diffraction mechanism Debye- sherrer as for the second called Automatic diffractometer of powders but one principle in both**[3]**.

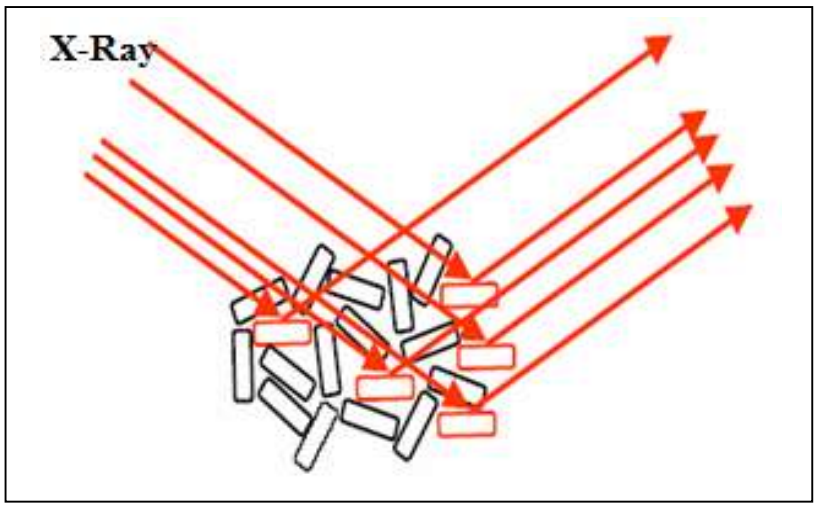

Figure (II.9): Better guidance for granules**[5]**.

- **Debye-Scherrer method:**

The Debye-Scherrer method is a way to determine the lattice constant of crystallised materials. A powdery crystalline sample is illuminated with monochromatic X-rays. The powder sample contains minute mono-crystals of about 5 - 50 μm diameter, so-called crystallites**[25]**.

This method relies on simple installation uses the bar from the film wraps around a cylinder called a camera or Debye – Scherrer room, where the sample placed on the camera axis and the incident beam is directed vertically to the powder. So the reflected rays form a cone which cuts the slide film in lines with half angle 2θ(The angle between the diffracted and primary ray). If we take into account the diffraction by the several families from levels, the result is a series of cones sharing the same summit and a form of diffraction as shown in figure(II-10)**[3]**.

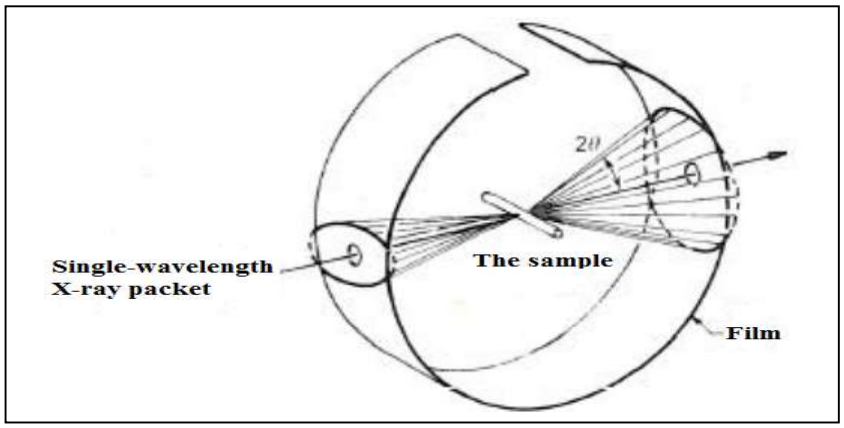

Figure (II.10): Debye-Scherrer method**[6]**.

But when we extend the slide, he diffraction takes the form of loops as shown in figure(II-11). Each half of the disc is made up on the sensitive film of a large number of small points, all the points coming from a single crystal, but this points are located close to each other so that they look as a line connected, and measures any line site on the film can set the value of θ and with knowing the value of the radiation wavelength λ can calculate the interlayer distance for these levels that made line. If R is the radius of the film, 2S is the distance between the two identical lines on the film then**[3,4,6]**:

$$2\theta = \frac{S}{R} \qquad \text{(II-4)}$$

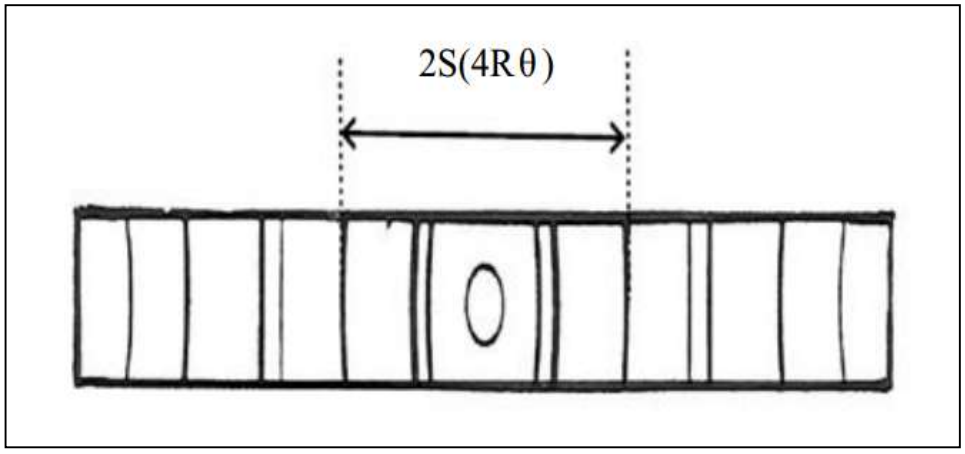

Figure (II.11): The form of loops obtained after the diffraction in the Debye-Scherrer way**[3]**.

- **Automatic diffractometer:**

There are several types of installation with different geometric configurations. The Bragg-Brentano method is most commonly used, and it is in this configuration that our samples were studied. The experimental setup is shown in Figure(II-12).

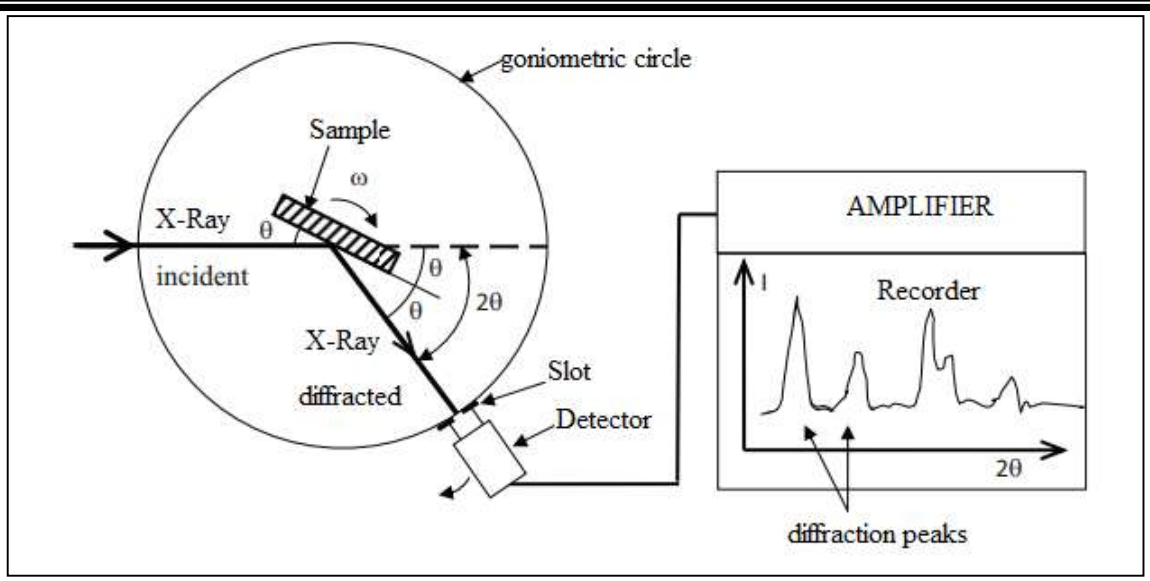

Figure (II.12): Diagram of operation of an X-ray automatic diffractometer**[26]**.

This arrangement comprises a tube in monochromatic X-rays, a sample carrier, an X-ray detector and a goniometer on which the detector moves. The incident X-rays emitted by the anticathode are diffracted by the sample. X photon detector measures the X-ray intensity as a function of the angle 2θ which it forms with the incident X-ray beam. The diffraction diagrams are therefore obtained called diffractograms that represent the intensity of diffracted photons depending to 2θ. Thus, using tables that exist in databases (ASTM records - American Society for Testing Materials), we can proceed with the identification of the phase and the lattice parameters corresponding to these diffractograms using a specific program and this what we'll do in the next chapter**[26]**.

Table (II.1): ASTM record for Barium Fluoride**[27]**.

04 - 0452					
BaF_2 **Barium Fluoride**	**d (Å)**	**I**	**h**	**k**	**l**
	3.579	**100**	**1**	**1**	**1**
	3.100	**30**	**2**	**0**	**0**
	2.193	**79**	**2**	**2**	**0**
	1.870	**51**	**3**	**1**	**1**
Rad.: Cu_{Ka1} I: 1.5406 Filter: Ni d-sp:	**1.790**	**3**	**2**	**2**	**2**
	1.550	**6**	**4**	**0**	**0**
Cut Off : Int. : Diffract. I/Icor. : 3.00	**1.423**	**13**	**3**	**3**	**1**
	1.386	**6**	**4**	**2**	**0**
Ref. : Swanson, Tatge, Natl. Bur. Stand. (U.S.) Circ.,	**1.266**	**14**	**4**	**2**	**2**

539,I,70 (1953)	1.1933	6	5	1	1
	1.0959	2	4	4	0
Sys. : Cubic S.G. : Fm3m (225)	1.0481	6	5	3	1
	1.0332	<1	6	0	0
a = 4.01270 b : c : A : C :	0.9803	2	6	2	0
a : b : g : Z : 4 mp :	0.9455	1	5	3	3
	0.9347	3	6	2	2
Ref. : Ibid	0.8948	1	4	4	4
Dx : 4.886 Dm : SS/FOM : F_{21}=84(.01119, 21)	0.8682	4	5	5	1
Color : Colorless	0.8599	1	6	4	0
Sample specially purified by Mallinckrodt. CAS #: 7787-32-8	0.8285	5	6	4	2
Fluorite group, fluorite subgroup. PSC: cF12. To replace 1-533,	0.8072	6	7	3	1
Mwt: 175.33, Volume [CD]: 238.34					

- **The refinement with le bail method:**

Le bail refinement is method that used for improving the crystal structure(the lattice parameters), this method aims to maximize the agreement between the calculated spectrum from the lattice parameters and the determined space group, and the experimental spectrum**[8]**.

The quality of the refinement is measured by agreement factors of weighted pattern (R_{wp}) and of pattern (R_p):

$$R_{wp}(\%)=100.\sqrt{\frac{\sum_i w_i.(y_{obs_i}-y_{calc_i})^2}{\sum_i w_i.(y_{obs_i})^2}} \quad \text{(II-5)}$$

$$R_p(\%)=100.\frac{\sum_i \left|y_{obs_i}-y_{calc_i}\right|}{\sum_i y_{obs_i}} \quad \text{(II-6)}$$

y_{obs_i} and y_{calc_i} being respectively the observed and calculated intensities at the i angular steps and w_i the weight assigned to the intensity at i angular steps.

The expected reliability factor R_{exp} (R- expected pattern) is given by:

$$R_{exp}(\%)=100.\left[\frac{N-P}{\sum_i w_i y_{obs_i}^2}\right]^{\frac{1}{2}} \quad \text{(II-7)}$$

Where N and P are the number of information used (measuring points) and the number of refined parameters respectively.

On other hand, the goodness-of-Fit(GoF) χ^2 is given by: $$\chi^2 = \left[\frac{R_{wp}}{R_{exp}}\right]^2 \quad \text{(II-8)}$$

The lattice parameters, profile functions diffraction lines and background noise are optimized with respect to the experimental spectrum to minimize agreement factors.

II.2 Scanning electron microscope/Energy dispersive spectroscopy (SEM/EDS):

Energy dispersive spectroscopy(EDS), also known as EDX(Energy Dispersive X-ray spectroscopy), coupled to the SEM is an analytical technique for determining the chemical composition of a sample examined via the qualitative and quantitative detection of these atomic elements. During EDS, a sample is exposed to an electron beam inside a scanning electron microscope (SEM). These electrons collide with the electrons within the sample, causing some of them to be knocked out of their orbits. The vacated positions are filled by higher energy electrons which emit x-rays in the process. By analyzing the emitted x-rays, the elemental composition of the sample can be determined. EDS is a very handy tool for performing the constitutional analysis of any kind of material. EDS is useful for the characterization of materials because it makes a qualitative and quantitative microanalysis on a specimen from a relatively low magnification (~ 25X) to a high magnification (~ 20000X).

The spectra of X-ray microanalysis are obtained having the characteristic lines of different intensities of the sample component elements, through the emitted radiation during the interaction between the incident electrons and the atoms of the sample(see Figure II-13) **[8,28,29]**.

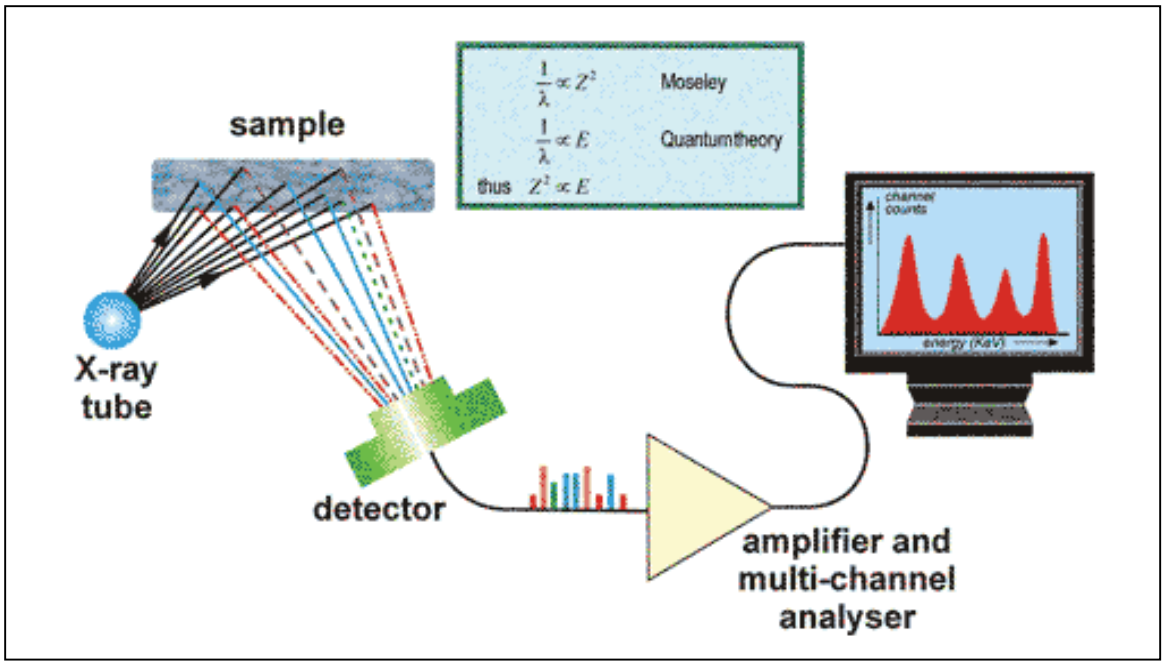

Figure (II.13): Energy Dispersive Spectrometer**[30]**.

The EDS technique select ratio of the elements presence in the compounds structure($Ca_{1-x}Sr_xFeO_{2.5}$) as shown in the table (II-2).

Table (II.2): The mass composition of $Ca_{0.3}Sr_{0.7}FeO_{2.5+y}$ compound by the theoretical calculation and analysis by EDS**[8]**.

The element	Ca	Sr	Fe
The theoretical composition(%)	7.11	36.25	33.01
The experimental composition(%)	7.59	36.88	36.30

The EDS appoints the oxygen ratio with great suspicion(see the figure II-14) and there are other devices of EDS with high technology determine the oxygen rate exactly but it is very expensive , so we must research about a mathematical method even we make it easier.

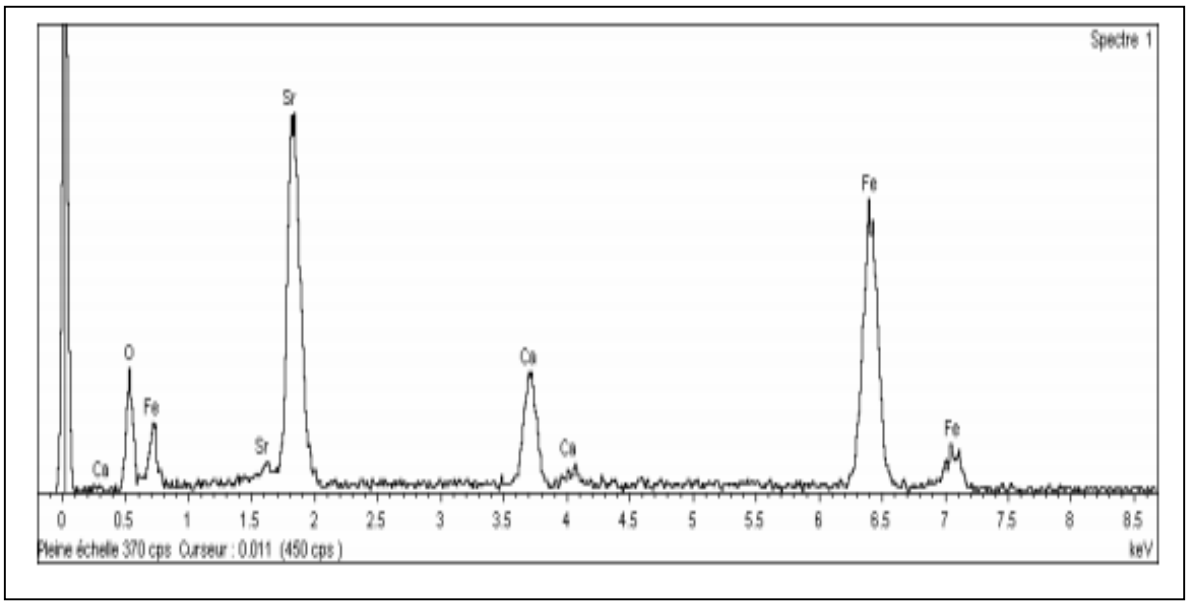

Figure (II.14): EDS spectrum of the $Ca_{0.3}Sr_{0.7}FeO_{2.5+y}$ sample**[8]**.

Conclusion :

We offered in this chapter Characterization techniques where we saw firstly definition of the x-ray diffraction, its production, and experimental methods for its diffraction, then we showed the principle and of EDS method.

Chapter III

The oxygen rate in the $Ca_{1-x}Sr_xFeO_{2.5+y}$ compounds (x=0.5; 0.7; 0.9)

III. The oxygen rate in the $Ca_{1-x}Sr_xFeO_{2.5+y}$ compounds (x=0.5; 0.7; 0.9):

Introduction:

X-ray diffraction phenomenon are of great importance in many fields, and it is the most commonly used in the world to determine the crystal structure of the various chemical compounds. Among the methods and experimental techniques that allows with identification of the crystal structure, we cite powder x-ray diffraction because the majority of crystalline solids are difficult to exist in the form of single crystals, and it is very expensive.

Many scientists developed their findings, using an automated programs to simulate these results and compare it with the theoretical data. Among these programs, we can cite:

Rex. Powder diffraction**[31]**, Maud, GSAS**[32]**, and FULLPROF program that will be used in this study to determine the lattice parameters for the $Ca_{0.1}Sr_{0.9}FeO_{2.5}$, using the refinement methods.

The $Ca_{1-x}Sr_xFeO_{2.5}$ compounds(x=0.5; 0.7) is studied in the past years, so we'll display its results directly.

Begin the study in this chapter by the sample preparation process in the form of powder from the $Ca_{0.1}Sr_{0.9}FeO_{2.5}$ compound, and then study by x-ray diffraction, the data are recorded and processed by the "le bail" refinement method and shows the resulting lattice parameters. In the last, we will calculates the oxygen rate in the $Ca_{1-x}Sr_xFeO_{2.5+y}$ compounds (x=0.5; 0.7; 0.90).

III.1 The XRD on the $Ca_{1-x}Sr_xFeO_{2.5}$ compounds(x=0.5; 0.7; 0.9):

III.1.1 Synthesis:

$Ca_{0.1}Sr_{0.9}FeO_{2.5}$ compound was prepared as a powder by the method of the solid solution, Stoichiometric amounts of $CaCO_3$ (Aldrich, 98%), $SrCO_3$ (Aldrich, 99.9% +) and Fe_2O_3 (Aldrich, 99% +) is mixed, then ground together in a mortar. The mixture was sintered in air at 1000 ° C for 12 hours in the oven. The powder was then ground and pressed into pellets. In each one of pellets of 13 mm in diameter is placed 1 g of this mixture. The pellets are sintered in the air in a conventional oven at 1200 °C for 24 hours, then dipped in liquid nitrogen. This operation is repeated several times. The reaction is described by the next chemical equation:

$$0.10CaCO_3 + 0.90SrCO_3 + \tfrac{1}{2}Fe_2O_3 \rightarrow Ca_{0.10}Sr_{0.90}FeO_{2.5} + \uparrow CO_2 \cdots (III\text{-}1)$$

III.1.2 The data recording:

To get the experimental diffractogramme of the studied compound, we put an amount of the $Ca_{0.1}Sr_{0.9}FeO_{2.5}$ compound powder wich prepared by the solid solution method in the diffractometer of the type Bruker D8 Advance as shown in the figure (III-1), in Bragg-Brentano configuration, using the copper radiation $K_{\alpha 1}$ (λ= 1.5406 Å) wich is fell to the powder and diffract through it. These diffracted rays is captured by the X-ray detector, this latter measures the X radiation intensity in terms of the 2θ angle as shown in the figure (III-2).

The diffractometer is controlled by a computer and coupled to a computer system that allows automatic exploitation of results.

Figure (III.1): Diffractometer of the type Bruker D8 Advance **[33]**.

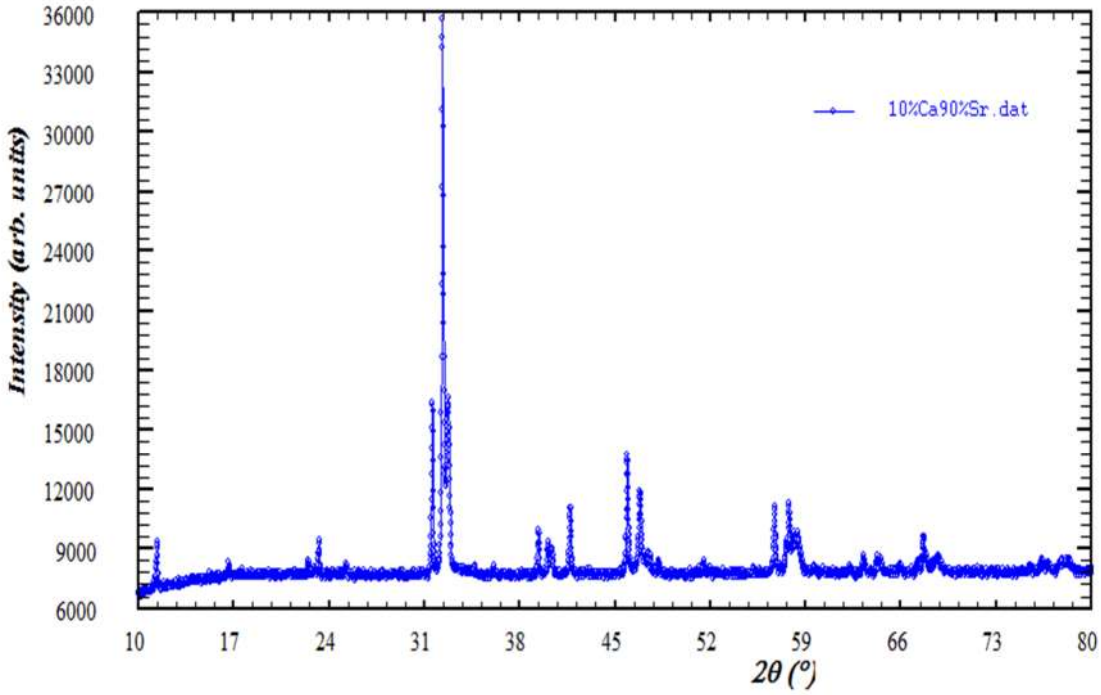

Figure (III.2): Powder diffractogramme of $Ca_{0.1}Sr_{0.9}FeO_{2.5}$ compound is obtained by the solid solution method.

III.1.3 The data processing:

It is known that $Sr_2Fe_2O_5$ and $Ca_2Fe_2O_5$ compounds forms the basis of the compounds composition with the general formula $Ca_{1-x}Sr_xFeO_{2.5}$, that the first compound crystallize in the *Imma* or *I2mb* space group, and *Pnma* for the second compound. This is mean that the $Ca_{0.1}Sr_{0.9}FeO_{2.5}$ compound is expected to crystallize in one of these three groups.

The *Imma* space group is characterized by the dynamic disorder case, which is attributed to irregular alternation of tetrahedral layers (Figure III.3) **[3, 4]**.

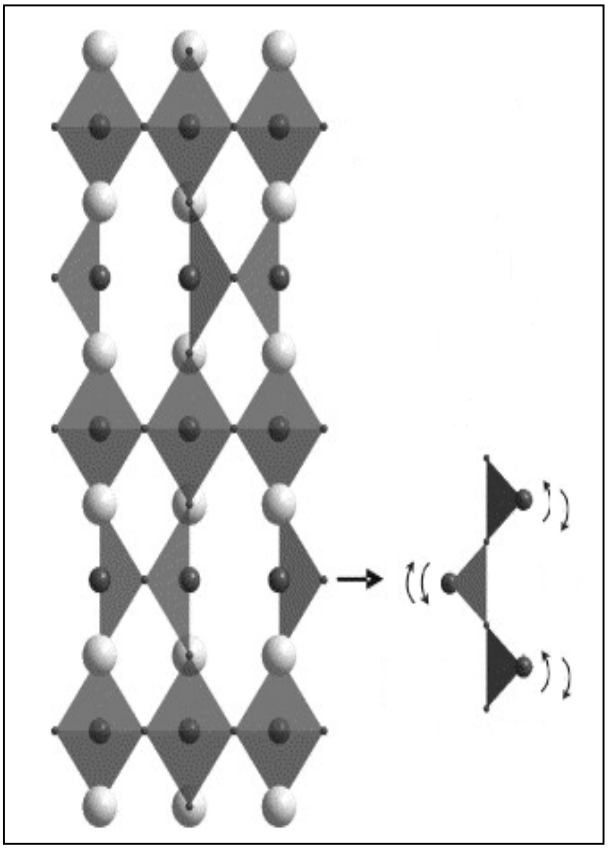

Figure (III.3): Description of the dynamic disorder case for the *Imma* group in the brownmillerite structure **[4]**.

Powder X-ray diffraction spectra are analyzed via FULLPROF program to determine the lattice parameters.

III.1.3.1 Refinements by using Le bail method:

In what follows, it is presented a description of $Ca_{1-x}Sr_xFeO_{2.5+y}$(x=0.5, 0.7, 0.9) compounds in each case:

- **$Ca_{0.5}Sr_{0.5}FeO_{2.5}$:**

It was the start with the lattice parameters mentioned by Nemudry et al. The values of these parameters are **[8]**:

a=5.4780Å, ***b***=15.2024Å and ***c***=5.6317Å

The following figure shows the refinement process for the $Ca_{0.5}Sr_{0.5}FeO_{2.5}$ compound:

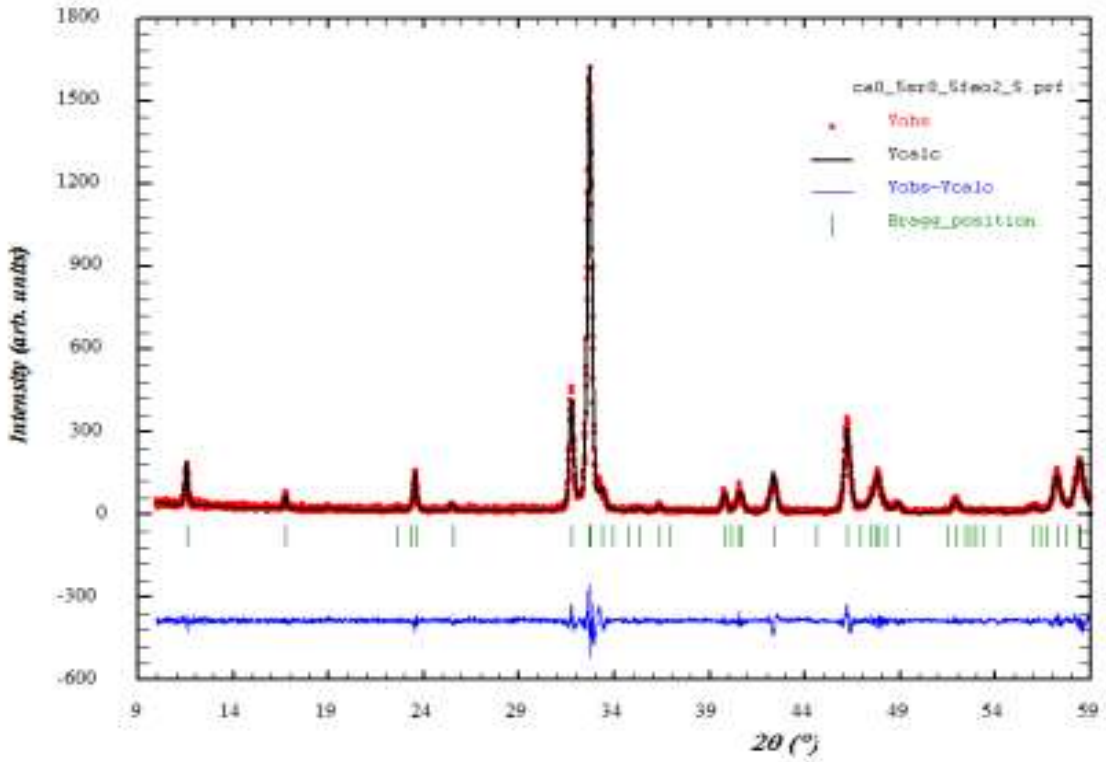

Figure (III.4): Refinement pattern of the powder x- ray diffraction for the $Ca_{0.5}Sr_{0.5}FeO_{2.5}$ compound**[8]**.

The measurement is in red, the refinement of le bail in black and the difference between the 2 blue. Green indicated the position of the lines.

- **$Ca_{0.3}Sr_{0.7}FeO_{2.5}$:**

For the purpose of refinement of this compound has been introduced the lattice parameters which is mentioned by Nemudry et al **[8]**. The values of these parameters are:

$$\boldsymbol{a}=5.4969\ \text{Å},\ \boldsymbol{b}=15.3524\ \text{Å and}\ \boldsymbol{c}=5.6465\ \text{Å}$$

The following figure shows the refinement process for the $Ca_{0.3}Sr_{0.7}FeO_{2.5}$ compound:

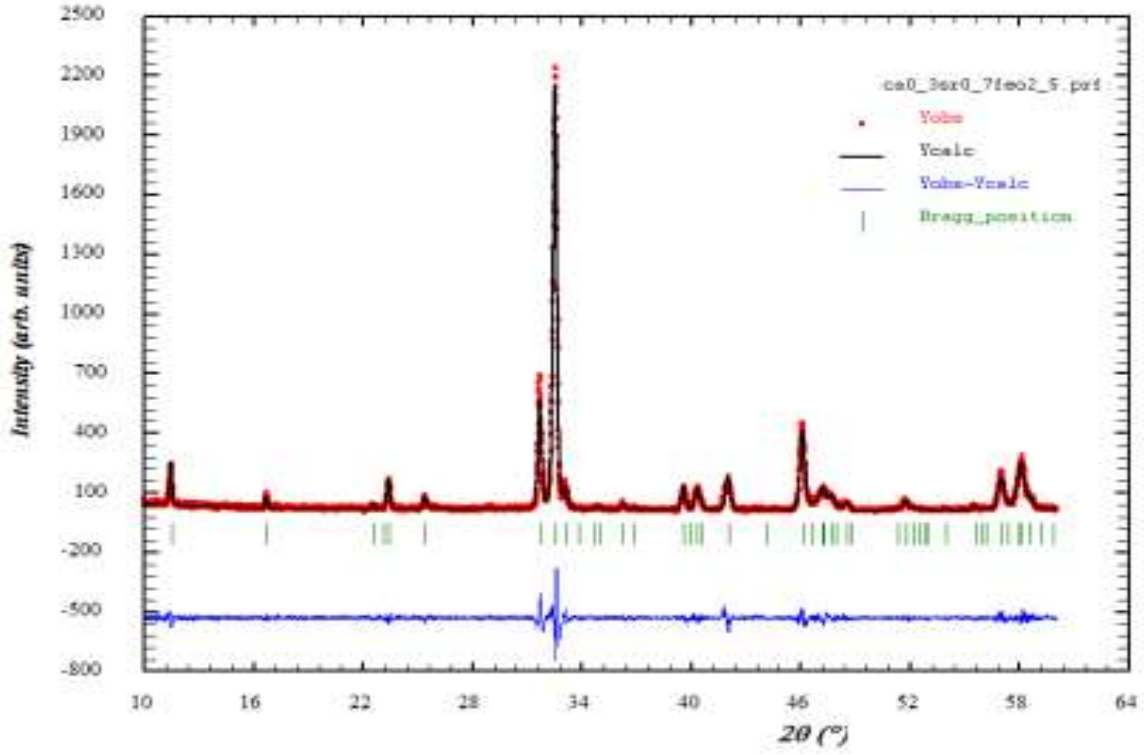

Figure (III.5): Refinement pattern of the powder x- ray diffraction for the $Ca_{0.3}Sr_{0.7}FeO_{2.5}$ compound**[8]**.

- **$Ca_{0.1}Sr_{0.9}FeO_{2.5}$:**

As a starting point for the refinement with "le bail" method, we have used the following lattice parameters: ***a***=5.503521 Å, b=15.501175 Å, ***c***=5.634557 Å

We get the figure below that χ^2=11.36 and this is in the orthorhombic space group *I2mb*.

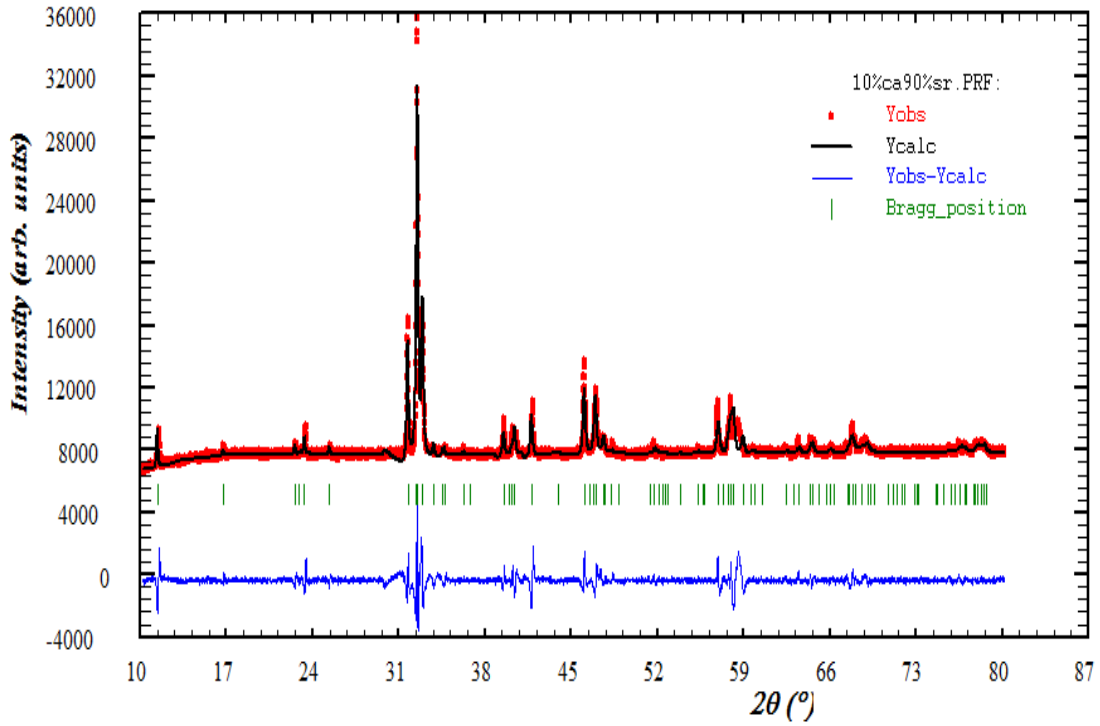

Figure (III.6): Refinement pattern of the powder x- ray diffraction for the $Ca_{0.1}Sr_{0.9}FeO_{2.5}$ compound.

- When we change the lattice parameters to the theoretical parameter values which is estimated with: ***a***=5.51584 Å, ***b***=15.50248 Å, ***c***=5.66138 Å, we get the figure below that χ^2=10.69 and this in the orthorhombic space group *I2mb*.

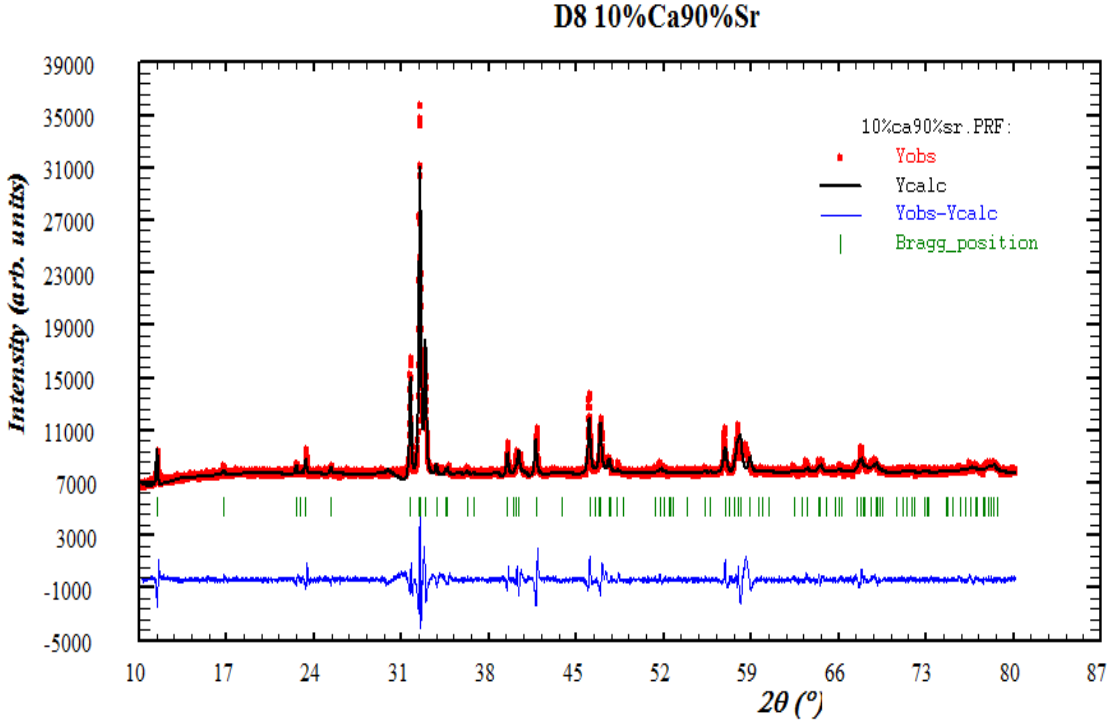

Figure (III.7): Refinement pattern of the powder x- ray diffraction for the $Ca_{0.1}Sr_{0.9}FeO_{2.5}$ compound when entering theoretical values of lattice parameters.

The refinement of diffractogrammes obtained by the X-ray given the lattice parameters listed in Table(III.1) below.

Table (III.1): Summary of lattice parameters for the different compounds ($Ca_{1-x}Sr_x FeO_{2.5+y}$)

x		*a*(Å)	*b*(Å)	*c*(Å)
0.5		5.47564	15.24293	5.62569
0.7		5.49172	15.38658	5.64041
0.9	**a**	5.50256	15.49773	5.63259
	b	5.50415	15.50551	5.63593

The a and b symbols back to the figures (III.6) and (III.7) respectively. And as the value of χ^2 in the b case is less than the a case, we will use the resulting lattice parameters for the second case in the calculation of next part.

III.2 Calculation of the oxygen rate in the $Ca_{1-X}Sr_XFeO_{2.5+y}$ compounds:

III.2.1 The Oxygen ions in the $Ca_{1-X}Sr_XFeO_{2.5}$ compounds:

In this part, we will clarify the presence of additional oxygen ions inside the compound structure by the comparison between the lattice parameters that we calculate the theoretical lattice parameters with the following relations and the lattice parameters related to $CaFeO_{2.5}$ and $SrFeO_{2.5}$ compounds are presented in the first chapter:

$$a_{theoretical} = (1-x) * a_{CaFeO_{2.5}} + (x) * a_{SrFeO_{2.5}} \ldots\ldots (III\text{-}2)$$

$$b_{theoretical} = (1-x) * b_{CaFeO_{2.5}} + (x) * b_{SrFeO_{2.5}} \ldots\ldots (III\text{-}3)$$

$$c_{theoretical} = (1-x) * c_{CaFeO_{2.5}} + (x) * c_{SrFeO_{2.5}} \ldots\ldots (III\text{-}4)$$

After the calculations, we display values of the theoretical lattice parameters in the tables below, and we will comparing them with the experimental values that we have acquired them through the x-ray diffraction.

Table (III.2): the lattice parameters of $Ca_{0.5}Sr_{0.5}FeO_{2.5}$ compound.

	Theoretical	**Experimental**
a	5.4753	5.47564
b	15.1731	15.24293
c	5.6334	5.62569

Table (III.3): the lattice parameters of $Ca_{0.3}Sr_{0.7}FeO_{2.5}$ compound.

	Theoretical	**Experimental**
a	5.4953	5.49172
b	15.33486	15.38658
c	5.64756	5.64041

Table (III.4): the lattice parameters of $Ca_{0.1}Sr_{0.9}FeO_{2.5}$ compound.

	Theoretical	**Experimental**
a	5.5153	5.50415
b	15.49662	15. 50551
c	5.66172	5.63593

Now, we calculate the difference between the theoretical and experimental lattice parameters for compare between them according to the following relations:

$$\Delta a=a_{exp}-a_{theo},\ \Delta b=b_{exp}-b_{theo},\ \Delta c=c_{exp}-c_{theo}\ldots\ldots \text{(III-5)}$$

Then, we display the results in the tables below.

Table (III.5): Difference between the lattice parameters of $Ca_{0.5}Sr_{0.5}FeO_{2.5}$ compound.

Δa	0,00034
Δb	0,06983

Δ*c*	-0,0077

Table (III.6): Difference between the lattice parameters of $Ca_{0.3}Sr_{0.7}FeO_{2.5}$ compound.

Δ*a*	-0,0036
Δ*b*	0,05172
Δ*c*	-0,0072

Table (III.7): Difference between the lattice parameters of $Ca_{0.1}Sr_{0.9}FeO_{2.5}$ compound.

Δ*a*	-0,0111
Δ*b*	0,00889
Δ*c*	-0,0258

Through the previous tables is clear that there is a difference between the theory and experimental lattice parameters at each value especially in value of '***b***', this indicates the presence of additional oxygen ions enter through the b axis, which we will calculates its percentage in the next point.

III.2.2 The calculation model:

After setting the lattice parameters values ***a***; ***b***; and ***c*** of the orthorhombic structure for series of $Ca_{1-x}Sr_xFeO_{2.5+y}$ compounds (x=0.5; 0.7; 0.9), we start a mathematical calculations, using the Excel program to set the percentage of oxygen in these compounds by searching for the value of "y".

III.2.2.1 The calculation steps:

- At first, we define the atomic packing factor (APF) which is the principle for calculating the oxygen percentage.

The atomic packing factor (APF) is the ratio of the atoms volume of the cell on the total volume which we can express about it with the following relation:

$$APF = \frac{The\ atoms\ number \times \frac{4}{3}.\pi.r^3}{The\ total\ volume\ of\ the\ cell} = \frac{n_i \times \frac{4}{3}.\pi.r^3}{V} \ldots\ldots \textit{(III-6)}$$

$$\rightarrow APF = \frac{n_i \times \frac{4}{3}.\pi.r^3}{a.b.c} \ldots\ldots\ldots\ldots (III\text{-}7)$$

Where:

APF: The atomic packing factor.

n_i: the atoms number.

r: Ionic radii[Å].

a, ***b***, ***c***: the lattice parameters[Å].

The previous relation of the atomic packing factor (APF) is in one kind of ions, if the compound have many kinds of ions, the relation become:

$$APF = \frac{n_1 \times \frac{4}{3}.\pi.r_1^3 + n_2 \times \frac{4}{3}.\pi.r_2^3 + \cdots}{a.b.c} \ldots\ldots\ldots (III\text{-}8)$$

Where n_1 and n_2 are the atoms number of the first and second ions respectively.

- We look at the coordination (closest neighbors) of the elements Ca; Sr; Fe and O, and then set its atomic and ionic radius using Shannon ionic radii for use it later in the mathematical calculations.

The following table shows values related to the $Ca_{1-x}Sr_xFeO_{2.5}$ compound ions that are needed in calculations.

Table (III.8): Information related to the $Ca_{1-x}Sr_xFeO_{2.5}$ structure.

Atom	Number in the cell	Coordination
Ca/ Sr	4	7
Fe(1)	2	4
Fe(2)	2	6
O(1)	4	4
O(2)	4	4
O(3)	2	4

- We have that: $Ca^{2+}_{1-x}Sr^{2+}_{x}Fe^{3+}O^{2-}_{2.5}$ is theoretical formula, and $Ca^{2+}_{1-x}Sr^{2+}_{x}Fe^{3+}O^{2-}_{2.5+y}$ is Experimental formula.
- In terms of experimental case reveals an amount 'y' make imbalance between the equation parties ,we take x=0.5 for example to clarify this imbalance:

$0.5\times2+0.5\times2+3=(2.5+y)\times(+2) \rightarrow 1+1+3=5+2y \rightarrow 5\neq5+2y$

So, to achieve the equality between the two equation parties. We suppose the presence of Fe^{4+} ions that the Fe^{3+} crystallize in the octahedral sites to the Fe^{4+} with loss one electron during a chemical reaction and the compound formula becomes:

$$Ca^{2+}_{0.5}Sr^{2+}_{0.5}Fe^{3+}_{1-x}Fe^{4+}_{x}O^{2-}_{2.5+y}$$

- We search for value of 'x' that achieve the equality as:

$0.5\times2+0.5\times2+(1-x)\times3+x\times4=(2.5+y)\times(+2) \rightarrow 1+1+3-3x+4x=5+2y \rightarrow 5+x=5=2y$

$\rightarrow x=2y$, So : $Ca^{2+}_{0.5}Sr^{2+}_{0.5}Fe^{3+}_{1-2y}Fe^{4+}_{2y}O^{2-}_{2.5+y}$

- After the calculation of the theoretical and experimental atomic packing factor (APF)as shown in the tables which is in the results part, we notice a difference between them which means presence an additional oxygen ions are calculated by appointing the value of 'y' when matching value of APF' $_{exp}$ with APF $_{theo}$.

The used relations in calculation of 'y' value are:

$$APF_{theo}=\frac{4\times(n_{Ca}\times\frac{4}{3}.\pi.r^3_{Ca}+n_{Sr}\times\frac{4}{3}.\pi.r^3_{Sr}+n_{Fe1}\times\frac{4}{3}.\pi.r^3_{Fe1}+n_{Fe2}\times\frac{4}{3}.\pi.r^3_{Fe2}+n_{O}\times\frac{4}{3}.\pi.r^3_{O})}{a\times b\times c};$$

$$APF_{exp}=\frac{4\times(n_{Ca}\times\frac{4}{3}.\pi.r^3_{Ca}+n_{Sr}\times\frac{4}{3}.\pi.r^3_{Sr}+n_{Fe1}\times\frac{4}{3}.\pi.r^3_{Fe1}+n_{Fe2}\times\frac{4}{3}.\pi.r^3_{Fe2}+n_{O}\times\frac{4}{3}.\pi.r^3_{O})}{a'\times b'\times c'};$$

And $$APF'_{exp}=\frac{4\times(n_{Ca}\times\frac{4}{3}.\pi.r^3_{Ca}+n_{Sr}\times\frac{4}{3}.\pi.r^3_{Sr}+n_{Fe1}\times\frac{4}{3}.\pi.r^3_{Fe1}+n_{Fe2(+3)}\times\frac{4}{3}.\pi.r^3_{Fe2(+3)}+n_{Fe2(+4)}\times\frac{4}{3}.\pi.r^3_{Fe2(+4)}+n_{O}\times\frac{4}{3}.\pi.r^3_{O})}{a'\times b'\times c'}.$$

Where nFe2(+4) is unknown value and uptake the value which we research about it, is 'y' value and nFe2(+3) is function for it: nFe2(+3)=0.5- nFe2(+4).

III.2.2.2 Results:

- **$Ca_{0.5}Sr_{0.5}FeO_{2.5+y}$:**

The results of this compound are presented in the table below.

Table (III.9): the calculation results of $Ca_{0.5}Sr_{0.5}FeO_{2.5+y}$ compound.

	Coordination	theoretical	experimental	experimental'
rCa	7	1,06	1,06	1,06
nCa		0,5	0,5	0,5
rSr	7	1,21	1,21	1,21
nSr		0,5	0,5	0,5
rFe1 (T)	4	0,49	0,49	0,49
nFe1		0,5	0,5	0,5
rFe2 +3 (O)	6	0,645	0,645	0,645
nFe2 (+3)		0,5	0,5	0,485
rFe2 +4 (O)	6	0,585	0,585	0,585
nFe2 (+4)		0	0	0,015
rO	4	1,38	1,38	1,38
nO		2,5	2,5	2,515
a		5,475	5,476	5,476
b		15,173	15,243	15,243
c		5,633	5,626	5,626
APF		0,2950	0,2937	0,2950

After the calculation with excel program and the matching between APF' $_{exp}$ and APF $_{theo}$, we get that: y=0,015, and the chemical formula becomes on the form: $Ca_{0.5}Sr_{0.5}FeO_{2.515}$.

- **$Ca_{0.3}Sr_{0.7}FeO_{2.5+y}$:**

The works about this compound produce the following:

Table (III.10): the calculation results of $Ca_{0.3}Sr_{0.7}FeO_{2.5+y}$ compound.

	Coordination	**theoretical**	**experimental**	**experimental'**
rCa	7	1,06	1,06	1,06
nCa		0,3	0,3	0,3
rSr	7	1,21	1,21	1,21
nSr		0,7	0,7	0,7
rFe1 (T)	4	0,49	0,49	0,49
nFe1		0,5	0,5	0,5
rFe2 +3 (O)	6	0,645	0,645	0,645
nFe2 (+3)		0,5	0,5	0,489
rFe2 +4 (O)	6	0,585	0,585	0,585
nFe2 (+4)		0	0	0,011
rO	4	1,38	1,38	1,38
nO		2,5	2,5	2,511
A		5,495	5,492	5,492
B		15,335	15,387	15,387
C		5,648	5,640	5,640
APF		0,2942	0,2932	0,2942

Calculations shows to : y= 0,011 and the chemical formula is: $Ca_{0.3}Sr_{0.7}FeO_{2.511}$.

- **$Ca_{0.1}Sr_{0.9}FeO_{2.5+y}$:**

The next table shows the result calculation of the $Ca_{0.1}Sr_{0.9}FeO_{2.5+y}$ compound .

Table (III.11): the calculation results of $Ca_{0.1}Sr_{0.9}FeO_{2.5+y}$ compound.

	Coordination	**theoretical**	**experimental**	**experimental'**
rCa	7	1,06	1,06	1,06
nCa		0,1	0,1	0,1
rSr	7	1,21	1,21	1,21
nSr		0,9	0,9	0,9
rFe1 (T)	4	0,49	0,49	0,49
nFe1		0,5	0,5	0,5
rFe2 +3 (O)	6	0,645	0,645	0,645
nFe2 (+3)		0,5	0,5	0,4981
rFe2 +4 (O)	6	0,585	0,585	0,585
nFe2 (+4)		0	0	0,0019
rO	4	1,38	1,38	1,38
nO		2,5	2,5	2,5019
a		5,515	5,504	5,504
b		15,497	15,506	15,506
c		5,662	5,636	5,636
APF		0,2934	0,2932	0,2934

When we used the calculation method as proposed in the previous part, we get: y=0,0019≈0.002, and the chemical formula is: $Ca_{0.1}Sr_{0.9}FeO_{2.502}$.

Conclusion :

In this chapter, our study are optimized about how to prepare the $Ca_{0.1}Sr_{0.9}FeO_{2.5}$ compound, and then studied by X-ray where the extracted information from the Automatic diffractometer is taken to be processed in the FULLPROF program by the "le bail" refinement method, and through our findings from the FULLPROF program, we have achieved a mathematical model that calculates the oxygen rate in the $Ca_{1-x}Sr_xFeO_{2.5+y}$ compounds (x=0.5; 0.7; 0.9).

General conclusion

General conclusion

The crystallography have an important applications especially in the solid oxide fuel cells, and is credited to development of the detection techniques on the crystalline structures as the X-ray diffraction which is one of the most important experimental methods to select the crystalline structures.

In this work, we gave an overview of the brownmillerite compounds which is related from the perovskite structures ABO_3, as we identified the (Ca, Sr)$FeO_{2.5}$ system belongs to the type of brownmillerite family and showing its lattice parameters. Among the used characterization techniques: Powder X-ray diffraction, EDS technique that it is important in determination the elements ratio in the studied compounds and it does not determine the presence ratio exactly of oxygen element which is essential to advance the application of SOFC.

In the context of trying to develop the materials that make solid oxide fuel cell electrolytes, we have identified the crystal structure of the studied compounds by x-ray diffraction on the powder, and then prepare the sample of powder with the solid solution method and placed in the Automatic diffractometer and we have registered the data and displayed it in the form of diffractogram, then come up the data processing step where we used the FULLPROF simulation program by the "le bail" refinement method which enabled us to extract the lattice parameters for the concerned compounds and then use it to find a mathematical model that calculates the oxygen rate in the series of $Ca_{1-x}Sr_xFeO_{2.5+y}$ compounds and verify its validation for the (x=0.5, 0.7, 0.9).

This work was limited only to the (x=0.5, 0.7, 0.9) compounds, while it should be noted that we can study the model validation on the rest compounds, which requires the need to continue the research, in addition the addressing to other techniques for characterization and determining the oxygen rate as Iodometry titration technique that can be the subject of new research in this field.

Appendix

Applications of brownmillerite's compounds

Applications of brownmillerite's compounds:

Introduction :

Fuel cells are among the most promising current energy alternatives thanks to their effectiveness and their positive impact on the environment plan. they have great potential to become the most effective clean technology to convert chemical energy into electrical energy and heat. In the case where the fuel is hydrogen, the global reaction of the fuel cell(the inverse reaction of the electrolysis of water) is:

$$H_2+1/2\ O_2 \rightarrow H_2O+heat \ldots\ldots\ldots\ldots(1)$$

The chemical reaction proceeds in an essentially composed of two electrode structure, the anode and the cathode, separated by an ion-conductive electrolyte as shown in the figure 1. A fuel cell consists of a stack of anode-electrolyte-cathode elements connected by an electronic conductor interconnexion of a material forming a stack(Figure 2)**[34]**.

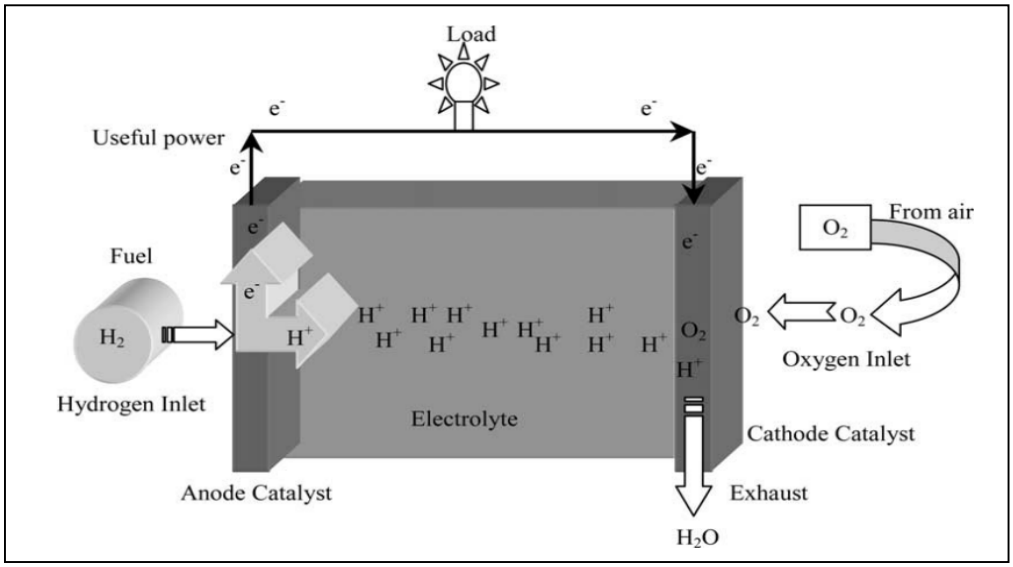

Figure (A.1): Typical fuel cell configuration **[35]**.

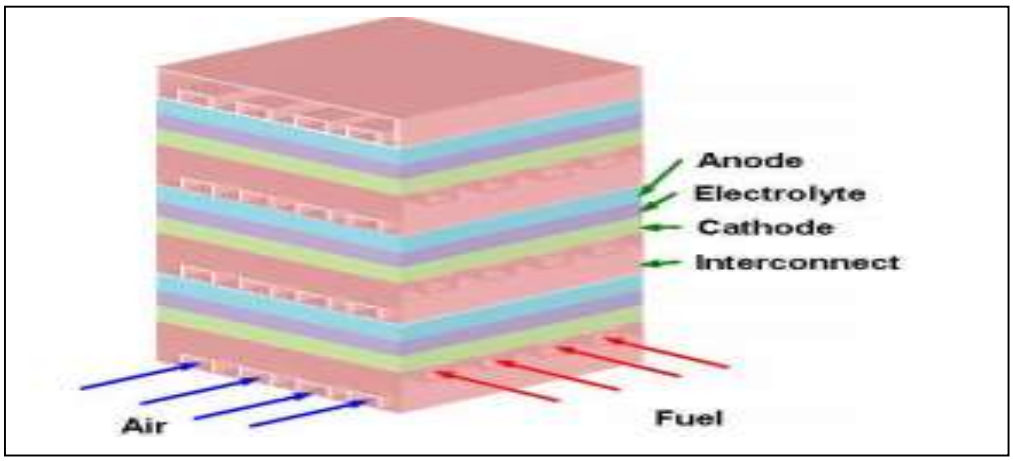

Figure (A.2): Photo of fuel cells stack**[36]**.

1- Types of Fuel Cells :

There are five major types of fuel cells, differentiated from one another by their electrolyte and the operating temperature:

- Alkaline fuel cell (AFC)
- Proton exchange membrane fuel cell (PEMFC)
- Phosphoric acid fuel cell (PAFC)
- Solid-oxide fuel cell (SOFC)
- Molten carbonate fuel cell (MCFC)**[34]**.

The table (A.1) summarizes the characteristics of various fuel cells.

Table (A.1): Main characteristics of fuel cells**[8, 37]**.

Type	**Phosphoric acid fuel cell(PAFC)**	**Alkaline fuel cell (AFC)**	**Proton exchange membrane fuel cell (PEMFC)**	**Molten carbonate fuel cell (MCFC)**	**Solid-oxide fuel cell (SOFC)**
Electrolyte	Phosphoric acid (liquid)	Potash (liquid)	Polymer (solid)	Molton salt such as nitrate, sulphate, carbonates (liquid)	Ceramic (solid)
Active ions	H^+	OH^-	H^+	CO_3^{2-}	O^{2-}
Temperature (°C)	160-200	60-90	80-110	600-800	500-1000
Combustible	Reformed H_2	H_2	Reformed H_2	Reformed H_2 /CO	Reformed H_2/CO/CH_4
Efficiency	~ 40%	~ 35%	~ 35%	>50%	>50%
Applications	Stationary	Space transport	Portable Transport Stationary	Stationary	Stationary, Transport

2- The basic elements of solid oxide fuel cell(SOFC):

SOFC technology holds the attention for the following reasons:

- Their high operating temperature (600 to 1000 ° C) necessary for obtaining a sufficient ionic conductivity of the ceramic electrolyte. At first this temperature allows the direct use of hydrocarbon. On other hand, it produces a heat in high temperature easily operable with or without cogeneration gas turbine;
- Is flexible in the choice of fuels, such as natural gas;
- Has a very long life potential (between 40 000-80 000 h);
- The contact between the two phases (gas-solid) reduces corrosion and eliminates all the problems of the electrolyte management;
- Their low CO_2 emissions (the CO_2 emitted by SOFCs from natural gas used as fuel to be reformed into hydrogen) and the absence of NO_x;
- Possibility of using carbon the monoxide CO as a fuel according to the following equation:

$$CO + O^{2-} \rightarrow CO_2 + 2e^- \text{ ……..(2)}$$

- No noise pollution due to the absence of mechanical parts**[8, 34]**.

3- Operating Principle of SOFC:

SOFCs differ in many respects from other fuel cell technologies. First, they are composed of all-solid-state materials. Second, the cells can operate at temperatures as high as 950 °C, significantly hotter than any other major category of fuel cell. Third, the solid state character of all SOFC components means that there is no fundamental restriction on the cell configuration.

A SOFC consists of two electrodes sandwiched around a hard ceramic electrolyte such as the remarkable ceramic material called zirconium. Hydrogen fuel is fed into the anode of the fuel cell and oxygen, from the air, enters the cell through the cathode. By burning fuel containing hydrogen on one side of the electrolyte, the concentration of oxygen is dramatically reduced.

The electrode on this surface will allow oxygen ions to leave the electrolyte and react with the fuel which is oxidized, thereby releasing electrons (e^-). On the other side of the plate, which is exposed to air, an oxygen concentration gradient is created across

the electrolyte, which attracts oxygen ions from the air side, or cathode, to the fuel side, or anode.

If there is an electrical connection between the cathode and the anode, this allows electrons to flow from the anode to the cathode, where a continuous supply of oxygen ions (O^{2-}) for the electrolyte is maintained, and oxygen ions from cathode to anode, maintaining overall electrical charge balance, thereby generating useful electrical power from the combustion of the fuel. The only by-product of this process is a pure water molecule (H_2O) and heat, as shown in figure 3**[37]**.

The SOFC reactions include:

Anode side :

$$2H_2 + 2O^{-2} \longrightarrow 2H_2O + 4e^- \ldots\ldots\ldots\ldots\ldots\ldots (3)$$

Cathode side:

$$O_2 + 4e^- \longrightarrow 2O^{-2} \ldots\ldots\ldots\ldots\ldots\ldots\ldots\ldots (4)$$

Total reaction:

$$2H_2 + O_2 \longrightarrow 2H_2O \ldots\ldots\ldots\ldots\ldots\ldots (5)$$

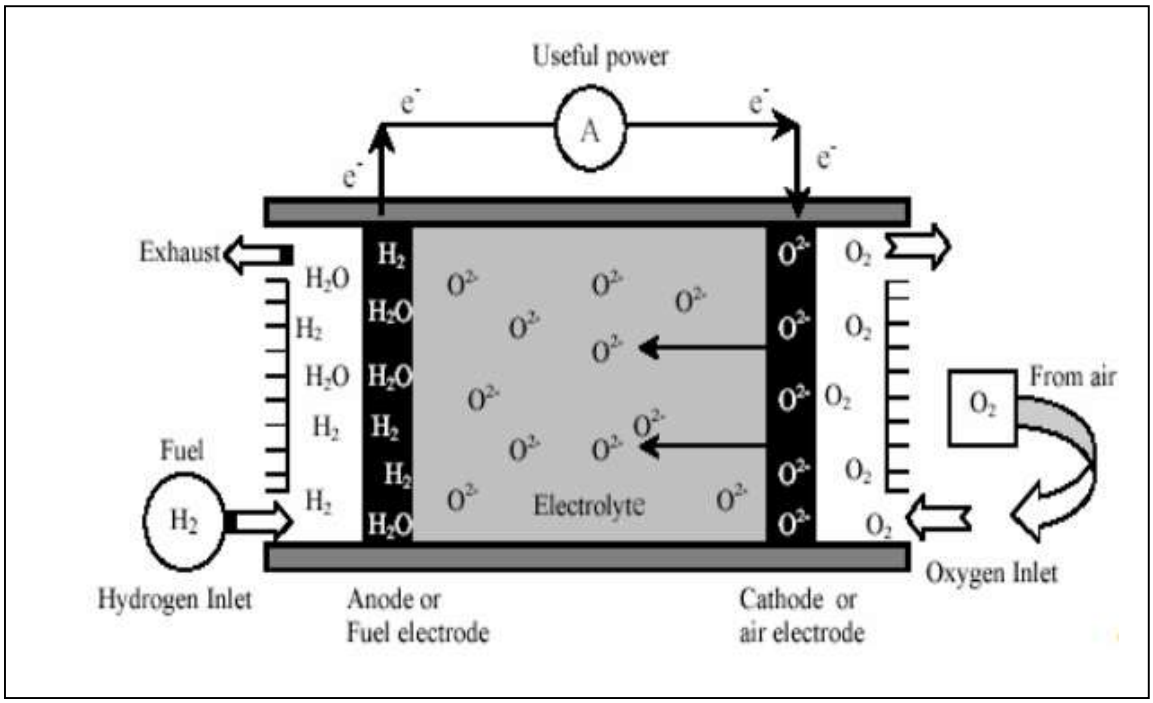

Figure (A.3): Solid Oxide Fuel Cell operating principle **[37]**.

3-1- Electrolyte :

Electrolyte is a material of solid oxide type have a high ionic conductivity to permit the migration of oxygen ions from the cathode to the anode, also have a low electronic conductivity to avoid the short circuit, and it have a good chemical stability. Electrolyte must be stable in the atmospheric pressure, and it characterized by the following properties:

- Ionic conductivity for the oxygen ions upward to 0.1 $S.cm^{-1}$ at 900 °C.
- Stability in large group from the partial pressure of oxygen($10^{-21} < P(O_2) < 0.21$ atm).
- It must have a coefficient of thermal expansion close to the poles coefficient.
- The good thermal and mechanical properties in order to carrying thermal shock.

Since the discovery of solid oxide fuel cells, the best electrolyte is stabilized yttrium zircon, it has high ionic conductivity consent to doping rate of 8% with Y_2O_3, and the main drawback of this matter is the lack of chemical stability compared with other components of the cell(anode and cathode), the thing that enjoined researchers find other materials for the manufacture of electrolyte are chemically stable, level with polar materials, which can meet the same specifications.

Research continued to reduce the degree of the cell operating temperature SOFC that was used the perovskites which containing lanthanum**[8,34,38]**.

3-2- Anode:

Anode is the seat of the reaction between hydrogen gas and the oxygen ions O^{2-}. The anode constituent materials must be stable in a reducing medium. The anode must have good electronic conductivity as well as good catalytic activity for the oxidation of fuel.

Thus the anode material must meet several conditions:

- Show high electronic conductivity, 10 to 100 $S.cm^{-1}$
- Have a dilation coefficient compatible with the other compounds of the cell.
- Be stable chemically until the partial pressions of oxygen in the order to 10^{-25} Pa.

High electrical conductivity associated with the need to operate under reducing atmosphere forced to use a metal as an anode. Different metals have been envisaged such as Ni, Pt, Ru…**[4].**

3-3- Cathode :

The cathode is the seat of the reduction reaction of oxygen, it is porous to allow gaseous oxygen to diffuse to the reaction point. The gas is adsorbed and then dissociated ions O^{2-} reduced through the presence of oxygen vacancies. The place where this reaction occurs and which are present simultaneously the electrons from the cathode, the electrolyte oxygen vacancies and oxygen gas is called triple point. This process is shown schematically in figure 4.

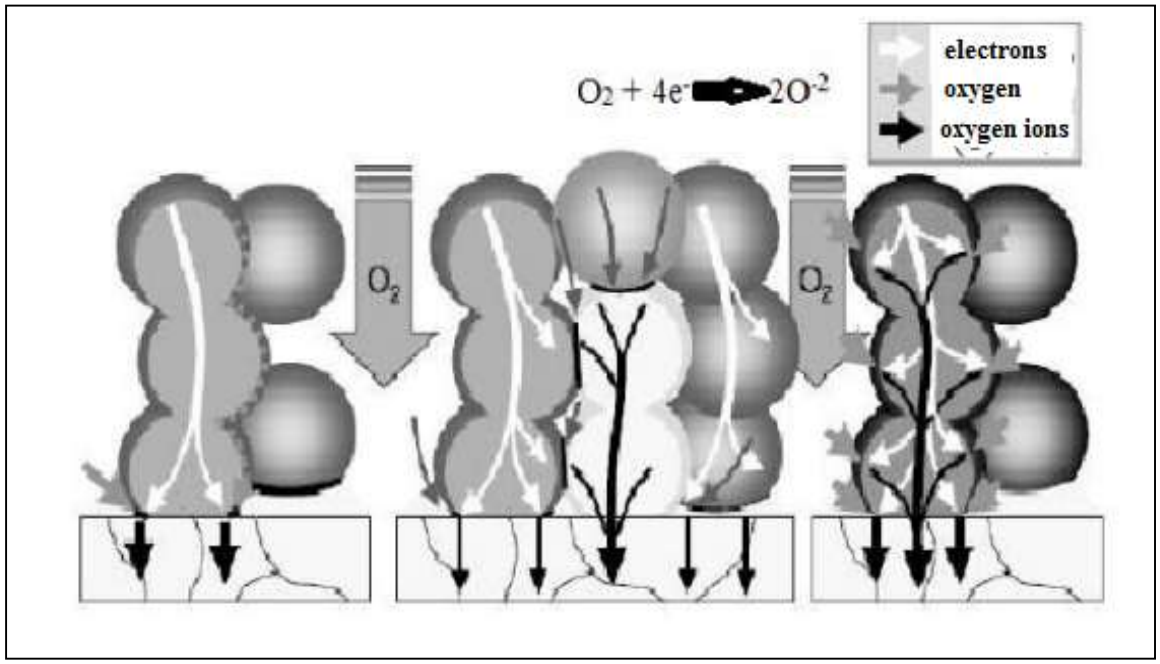

Figure (A.4): Various transport phenomena and the incident interaction in the cathode**[4]**.

The specifications generally admitted for the cathode material is:

- Have high electrocatalytic activity for reducing oxygen and high electrical conductivity(>100 $S.cm^{-1}$).
- Have good chemical stability, morphological and dimensional in the oxidizing environment.
- Have good mechanical and chemical compatibility with other cell components, chemical interaction or inter-diffusions elementary between the cathode and the adjacent components must be limited in order to minimize the occurrence of non-conductive secondary phases, expansion coefficient of changes and the introduction of electron conduction in the electrolyte**[8,34]**.

References

[1] فاطمة بلقاضي، مريم سعيدي،"الطاقات المتجددة"، مذكرة تخرج لنيل شهادة أستاذ التعليم الثانوي، المدرسة العليا للأساتذة، القبة القديمة، الجزائر(2004).

[2] Y.Sekiou, "Dimensionnement d'une installation de production d'hydrogène photovoltaïque dans la région de Ouargla", Mémoire master académique, Universités Kasdi merbah, Ourgla(2013).

[3] ك. بكاكرة، "دراسة تأثير درجة الحرارة في المركب $Ca_{0.95}Sr_{0.05}FeO_{2.5}$ "، مذكرة ماستر، جامعة الوادي، الجزائر، (2015).

[4] ف. فقير، "دراسة ظاهرة النقل الأيوني في المركب $SrFeO_{2.5}$"، مذكرة ماستر، جامعة الوادي،الجزائر، (2014).

[5] س. تامة، "تحضير و تحديد البنية البلورية بواسطة انعراج الأشعة السينية على المسحوق للمركب $Ca_{0.3}Sr_{0.7}FeO_{2.5}$"، مذكرة ماستر، جامعة الوادي، الجزائر، (2013).

[6] س. حريز بالقاسم، "تحديد البنية البلورية للمركب $Ca_{0.5}Sr_{0.5}FeO_{2.5}$ باستعمال انعراج الأشعة السينية"، مذكرة ماستر، جامعة الوادي،الجزائر، (2013).

[7] Antonio Diego Lozano-Gorrín, "Structural Characterization of New Perovskites", Polycrystalline Materials- Theoretical and Practical Aspects, Prof. Zaharii Zakhariev (Ed.), ISBN: 978-953-307-934-9,

[8] M. S. MAHBOUB, "Synthèse, caractérisation par diffraction X et spectroscopie raman des composés $Ca_{1-x}Sr_xFeO_{2.5-\delta}$ (δ =0, 0.5)", Thèse doctorat, Université mentouri, Constantine, Algérie, (2012).

[9] Mme LAMRANI Epouse AMOUAZ Nouara, "Synthèse et caractérisation de matériaux diélectrique a structures perovskite complexe de type $Ca_{1-x}A_xTi_{1-y}B_yO_3$(A=Sr, B=Zr,…)" , Thèse doctorat, Université Mouloud mammeri, Tizi-Ouzou, Algérie, (2011).

[10] F. Lindberg, "Studies of oxygen deficient complex cobaltates with perovskite related structures", Doctoral thesis, Stockholm university, Sweden, (2006).

[11] R. Le Toquin, "Réactivité, structure et propriétés physiques de $SrCoO_{2.5+\delta}$ et $La_2CoO_{4.0+\delta}$ étude par diffraction des rayons x et des neutrons in situ", Thèse de doctorat, Université de Rennes1, France, (2003).

[12] P. Berastegui; S.-G. Eriksson, S. Hull, *Mater. Res. Bull.* 34, 303-314,(1999).

[13] G.J. REDHAMMER, G.TIPPELT, G.ROTH, G.AMTHAUER, *American Mineralogist*. 89, 405-420, (2004).

[14] س. بضياف، "دراسة التركيب الجزيئي لرمال كثبان منطقة ورقلة باستخدام مطيافية الامتصاص ما تحت الأحمر و حيود الأشعة السينية"، مذكرة ماستر، جامعة قاصدي مرباح، ورقلة، الجزائر، (2012).

[15] I. BOUDRAA, "Synthèse et étude structurale par diffraction des rayons X desphosphates mixtes des métaux à valences II, III et V ", Mémoire de magister, université mentouri, Constantine, Algérie, (2010)

[16] مسعودة نصيري، "استعمال البرنامج Fullprof لتحديد البنية البلورية للمركب $CaFeO_{2.5}$ "، مذكرة ماستر، جامعة الوادي، الجزائر، (2012).

[17] H. Litiem, "Caractérisation avec Rayonnement X des Revêtements Durs Sur des Substrats en Acier", Mémoire de master, Université KASDI MERBAH, OUARGLA, Algérie, (2012).

[18] I. RAHIL, "ÉLABORATION ET CARACTERISATION DE REVÊTEMENTS DURS Mo-Cr et Mo-Cr-N", Mémoire de magister, Université Mentouri, Constantine, Algérie, (2008).

[19] M. ABBA, " Synthèse, caractérisation et étude Des propriétés Piézo-électriques des céramiques de type PZT: $Pb_{1-y}\ La_y\ [Zr_x\ Ti_z\ (\ Mo_{1/3}\ In_{2/3}\ )_{1-(x\ +z)}\ ]_{1-y/4}\ O_3$", Thèse de doctorat, Université Mohamed Khider, Biskra, Algérie, (2013).

[20] ع. نعيمة، م. سليمان، "علم البلورات والأشعة السينية"، دار الفكر العربي، مصر، (2005).

[21] أ. حرابي، "دراسة الخصائص الفيزيائية و النشاط الحيوي للهيدروكسيأباتيت الطبيعي $Ca_{10}(PO_4)_6(OH)_2$"، مذكرة ماجستير، جامعة منتوري قسنطينة، الجزائر، (2009).

[22]أ.د.يسري مصطفى، فيزياء الحالة الصلبة، الجزء الأول، منشورات دار الأكاديمية للطباعة و التأليف و الترجمة و النشر، 2007،ليبيا.

[23] أ.د.محمد أمين سليمان- أ.د.أحمد فؤاد باشا- أ.د.شريف أحمد خيري، فيزياء الجوامد، دار الفكر العربي، الطبعة الأولى، 2010،مصر.

[24] http://www.xtal.iqfr.csic.es/Cristalografia/parte_06-en.html, 30-04-2016.

[25] http://www.ld-didactic.de/literatur/hb/e/p7/p7124_e.pdf, 05-05-2016.

[26] T. Brouri, "Elaboration et étude des propriétés électriques des couches minces et des nanofils de ZnO", Thèse de doctorat, Université Paris-Est, France, (2011).

[27] http://ressources.univ-lemans.fr/acceslibre/um/pedago/chimie/06/deug/chim210b/baf2.html, 04-05-2016.

[28] M. KUMAR, Sh. S. Sahu, "Zinc Oxide Nanostructures Synthesized by Oxidization of Zinc", Bachelor of Technology thesis, Deemed University, Orissa, India, (2010).

[29] D. Fofanov, "Synthesis, characterization and physical properties of metal borides", doctoral thesis, Hamburg university, Germany, (2006).

[30] http://www.machinerylubrication.com/Read/602/xrf-oil-analysis, 06-05-2016.

[31] M. Bortolotti, L. Lutterotti and I. Lonardelli, *ReX:" a computer program for structural analysis using powder diffraction data",* J. Appl. Cryst. (2009) 42, 538-539.

[32] LUCA LUTTEROTTI, "*introduction to diffraction and the Rietveld method*", laboratoritio scienza e tecnologia dei materiali (2012).

[33] http://www.bgtu.net/eng/rfa/, 20-03-2016.

[34] Malika Diafi, "Synthèse et propriétés physiques d'oxyde mixtes à base de lanthane calcium et aluminium", Thèse Doctorat, Université Mohamed Khider, Biskra, Algérie,(2013).

[35] A. Boudghene Stambouli ; E. Traversa, "Fuel cells, an alternative to standard sources of energy", renewable and sustainable energy reviews 6, 297–306, (2002).

[36] Navadol Laosiripojana ; wisitsree wiyarath ; worason kiatkittpong; Arnornchai Arprornwichanop; Apinam sottitantawat; sattichai assabumrungrat, "Reviews on solid oxide fuel cells", ENGINEERING JOURNAL : VOLUME 13, 65-83, (2009).

[37] A. Boudghene Stambouli and S. Djerroud, "Thin film Si solar cell and solid oxide fuel cell technologies for a low cost, environmentally friendly and sustainable source of energy", Revue des Energies Renouvelables Vol. 14 N°2 , 267 – 284, (2011).

[38] Soumaia ABBES , "Study of Operating Conditions of the Polymer Electrolyte Membrane Fuel Cell (PEMFC) ", Master thesis, University of El-oued, (2012).

Abstract :

This work presents a study about calculation of the oxygen rate in the $Ca_{1-x}Sr_xFeO_{2.5+y}$ brownmillerite compounds (x=0.5; 0.7; 0.9) based on the determination of its lattice parameters by x-ray powder diffraction from sample synthesized by solid solution method.

Diffractogrammes were processed using the FULLPROF software depends on the "le bail" refinement, where we have arrived to achieving a mathematical model to estimate the oxygen rate through calculating its atomic packing factor(APF) which is the ratio of the atoms volume of the cell on the total volume.

Keywords: Atomic packing factor(APF), Brownmillerite, $Ca_{1-x}Sr_xFeO_{2.5+y}$, FULLPROF software, oxygen rate .

Résumé:

Ce travail présente une étude sur le calcul du taux d'oxygène dans les composés brownmillerite $Ca_{1-x}Sr_xFeO_{2.5+y}$ (x=0.5; 0.7; 0.9) basés sur la détermination de ses paramètres de maille par la diffraction des rayons X sur poudre synthétisés par la méthode de solution solide. Les diffractogrammes ont été traitées à l'aide du logiciel de FULLPROF basés sur la méthode d'affinement "le bail", où on a arrivés à la réalisation d'un modèle mathématique permet d'estimer le taux d'oxygène à travers le calcul de ces compacités qui est le rapport de la somme des volumes des atomes de la maille au volume total de la maille étudiée.

Les mots clés: Compacité, Brownmillerite, $Ca_{1-x}Sr_xFeO_{2.5+y}$, FULLPROF, taux d'oxygène.

ملخص:

يقدم هذا العمل دراسة حول حساب نسبة الأوكسجين في مركبات البرونمليريت $Ca_{1-x}Sr_xFeO_{2.5+y}$ (x=0.5 ; 0.7 ; 0.9) إنطلاقا من تحديد ثوابت الشبكة لها عن طريق إنعراج الأشعة السينية على المساحيق وذلك بتحضير العينة بطريقة المحلول الصلب و باستخدام جهاز الانعراج الآلي الذي أعطى مخططات انعراج تمت معالجتها باستعمال برنامج FULLPROF الذي يعتمد على طريقة التحسين لـ Le Bail، حيث تم التوصل إلى تحقيق نموذج رياضي يحسب لنا نسبة الأوكسجين في هذه المركبات من خلال حساب نسبة التعبئة الحجمية لها والتي هي مساوية لحجم الذرات على الحجم الكلي للخلية.

الكلمات المفتاحية: نسبة التعبئة الحجمية، البرونميليريت، $Ca_{1-x}Sr_xFeO_{2.5+y}$، FULLPROF، نسبة الأوكسجين.